Document Number: H2020-EUK-815323/5G-ALLSTAR/D3.2

Project Name:
5G AgiLe and fLexible integration of SaTellite And cellulaR (5G-ALLSTAR)

Deliverable D3.2

Interference analysis for terrestrial-satellite spectrum sharing

Date of delivery: 31/12/2019
Version: 0.1
Start date of Project: 01/07/2018
Duration: 36 months

Deliverable D3.2
Interference analysis for terrestrial-satellite spectrum sharing

Project Number:	H2020-EUK-815323
Project Name:	5G AgiLe and fLexible integration of SaTellite And cellu-laR

Document Number:	H2020-EUK-815323/5G-ALLSTAR/D3.2
Document Title:	Interference analysis for terrestrial-satellite spectrum sharing
Editor(s):	Leszek Raschkowski (FhG-HHI)
Authors:	Gosan Noh (ETRI), Leszek Raschkowski (FhG-HHI), Stephan Jaeckel (FhG-HHI), Nicolas Cassiau (CEA) Additional authors from Chungnam National University under subcontract agreement with ETRI: Bang Chul Jung, Jeong Seon Yeom
Dissemination Level:	PU
Contractual Date of Delivery:	31/12/2019
Security:	Public
Status:	Draft
Version:	0.1
File Name:	5G-ALLSTAR_D3.2 Interference analysis for terrestrial-satellite spectrum sharing_AG.docx

Abstract

This deliverable has been created as part of the work in the project 5G-ALLSTAR Work Package 3 (WP3) on Spectrum Sharing. It reports the findings of the interference analysis for terrestrial-satellite spectrum sharing by using different approaches for the co-channel interference such as outage probability based, stochastic geometry-based, QuaDRiGa based and ray-tracing based, in addition to an interference analysis of the adjacent channel interference. Possible interference situations are described and certain situations are selected for the analyses.
The selected interference situations can be further shortlisted based on the findings of this report, in order to increase the focus on the most severe cases for the following task of designing interference mitigation techniques.

Keywords

Spectrum, frequency bands, channel model, ray-tracing, quadriga, non-terrestrial, dual-connectivity, 5G, interference analysis, satellite

Acknowledgements

We would like to acknowledge the following people for the valuable reviews to the deliverable:
Guido Casati (FhG-IIS)
Alessandro Giuseppi (CRAT)
You-Jun Choi (KATECH)
We would also like to acknowledge and thank the assistance of Prof. Ke Guan's team at Beijing Jiaotong University.

Executive Summary

This deliverable presents the findings of the interference analysis for terrestrial-satellite spectrum sharing. It discusses possible interference situations and selects the most important cases for the analyses. In general, it can be differentiated between the interference that is caused by the non-terrestrial system onto the terrestrial system and the interference that is caused by the terrestrial system onto the non-terrestrial system. Further, the interference can be categorized into co-channel and adjacent channel interference.

The analysis of co-channel interference is based on the channel models that were developed in the beginning of the project. In addition, an outage probability analysis and a stochastic geometry-based analysis was conducted.

The theoretically derived outage probability analysis for the considered scenarios could be verified by simulations. The stochastic geometry-based analysis investigates the interference caused by terrestrial base stations (BSs) onto the satellite earth stations (SESs) based on antenna orientation of the SES and the distance between these nodes.

The ray-tracing based analysis investigates the impact of rain onto the interference at satellite UEs and cellular UEs caused by terrestrial BSs and satellites, respectively. In addition, the geometric-stochastic approach based on QuaDRiGa examines the interference situations also in two frequency bands that are currently envisaged for the deployment of a satellite 5G system, i.e. S-band and Ka-band.

Finally, the adjacent channel interference analysis studies the need for additional signal processing at the waveform level in order to mitigate interference at satellite UE caused by terrestrial gNBs.

Contents

List of Figures

List of Tables

List of Abbreviations

2D	2 Dimensions / 2-Dimensional
3D	3 Dimensions / 3-Dimensional
3GPP	3rd Generation Partnership Project
ARQ	Automatic Repeat Request
AWGN	Additive White Gaussian Noise
CA	Carrier Aggregation
CDF	Cumulative Distribution Function
CIR	Carrier-to-Interference Ratio
CNIR	Carrier-to-Noise-and-Interference Ratio
CNR	Carrier-to-Noise Ratio
CP-OFDM	Cyclic-Prefix OFDM
DL	Downlink
FSS	Fixed Satellite Service
GEO	Geostationary Earth Orbit
GF	Geometry Factor
HARQ	Hybrid ARQ
IoT	Internet of Things
ISD	Inter-site distance
LEO	Low Earth Orbit
LOS	Line-Of-Sight
MEO	Medium Earth Orbit
MSS	Mobile Satellite Service
NLOS	Non-Line-Of-Sight
OFDM	Orthogonal Frequency Division Multiplexing
PDF	Probability Density Function
PG	Path Gain
QoS	Quality of Service
RTT	Round Trip Time
Rx	Receiver
SES	Satellite Earth Station
SINR	Signal-to-Interference-and-Noise Ratio
SIR	Signal-to-Interference Ratio
SNR	Signal-to-Noise Ratio
TBD	To Be Decided
Tx	Transmitter
UE	User Equipment
UL	Uplink
VSAT	Very Small Aperture Terminal

1 Introduction

The introduction of spectrum sharing techniques between terrestrial and satellite systems requires investigations in the interference that these systems cause to each other. In case of severe inference, mitigation strategies have to be put in place in order to support the 5G-ALLSTAR vision of a mobile communication network that comprises a terrestrial radio access as well as a satellite radio access part.

In Section 2, the report first discusses the interference situations that are considered in this project. Types of interferers and victims are introduced and the interference categorization into co-channel and adjacent channel interference is motivated.

A small introduction about metrics commonly used in interference analyses is given in Section 3, in addition to some more general assumptions in the context of non-terrestrial networks.

The main part of the document (Section 4) focuses on the analysis of co-channel interference utilizing the channel models that were developed in the beginning of the project and are described in [27]. Both developed models, i.e. the ray-tracing based channel model and the stochastic geometry-based channel model (QuaDRiGa) are used for this purpose. In addition, the outage probability is analysed based on a theoretical approach.

Finally, the adjacent channel interference is analysed in Section 5, assuming a Cyclic-Prefix Orthogonal Frequency Division Multiplexing (CP-OFDM) system considering the 5G New Radio (NR) numerology as well as 5G NR Modulation and Coding Schemes (MCSs).

2 Considered interference situations

2.1 Interferer and victim types

The interference of interest that shall be investigated occurs between satellite (i.e., non-terrestrial) and cellular (i.e., terrestrial) communication systems. The satellite can be either Geostationary Earth Orbit (GEO) or Low Earth Orbit (LEO) satellites, summarized as follows:

- GEO satellites are located in a geostationary orbit (at an altitude of 35,786 km in the equatorial plane), and are seen from the Earth as if they are fixed in a specific location in the sky since the angular velocities of the Earth's self-rotation and the satellite match. Hence, there is no Doppler shift induced by the satellite motion.
- LEO satellites rotate around the Earth at a much lower orbit (less than 2,000 km), and are seen to be moving fast from the Earth's view (at an orbital period of a few hours) [5], leading to very high Doppler shift even for the stationary UE on the ground. The Doppler shift value depends on several factors: carrier frequency, Earth radius, satellite altitude, and satellite angular velocity. Due to the above effects, the interference from/to LEO is much more intense and dynamic compared to its GEO counterpart.

The system consists of base stations (BSs), UEs, satellites (Sats) and Satellite Earth Stations (SESs). Possible interference situations are shown in the following table.

Table 2-1: Considered interference cases

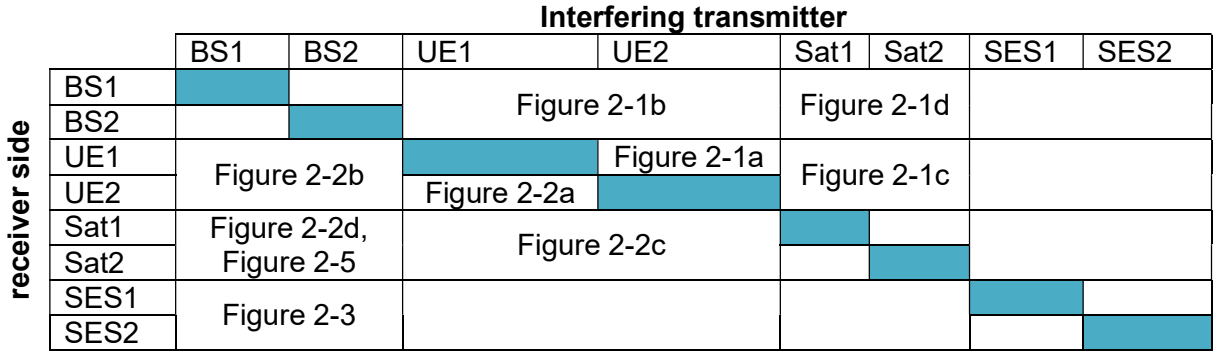

Legend: Self-interference

The first interference type is the satellite-to-cellular interference, i.e. interference from satellite devices to cellular devices. As shown in Figure 2-1, more specific classification is possible in terms of interferer and victim. The interferer can be either a satellite UE (a UE that is served by a satellite), as shown in Figure 2-1a and Figure 2-1b, or a satellite itself, as shown in Figure 2-1c and Figure 2-1d. The victim can be either a cellular UE (a UE that is served by the terrestrial system), as shown in Figure 2-1a and Figure 2-1c, or a cellular gNB, as shown in Figure 2-1b and Figure 2-1d. Summarizing the above, there are four specific scenarios regarding the interference from the satellite link to the cellular link:

- Interference from satellite UE to cellular UE is shown in Figure 2-1a. This scenario occurs when the satellite link operates in the uplink direction while the cellular link operates in the downlink direction. The interference distance can be short, potentially leading to a significant impact to a cellular UE if the beam directions are aligned with each other.

- Interference from a satellite UE to a cellular gNB is depicted in Figure 2-1b. This scenario occurs when both the satellite and cellular links operate in the uplink. The interference distance can be short, potentially causing a significant interference onto the cellular gNB.
- Interference from satellite to cellular UE as depicted in Figure 2-1c. This scenario occurs when both the satellite and cellular links operate in the downlink. Due to a much longer distance of the satellite link, it is expected that the interference experienced by the cellular UE will be not significant.
- Interference from satellite to cellular gNB as depicted in Figure 2-1d. This scenario occurs when the satellite link operates in the downlink direction while the cellular link operates in the uplink direction. Similar to the above case, the interference will not be significant due to the much longer distance of the satellite link.

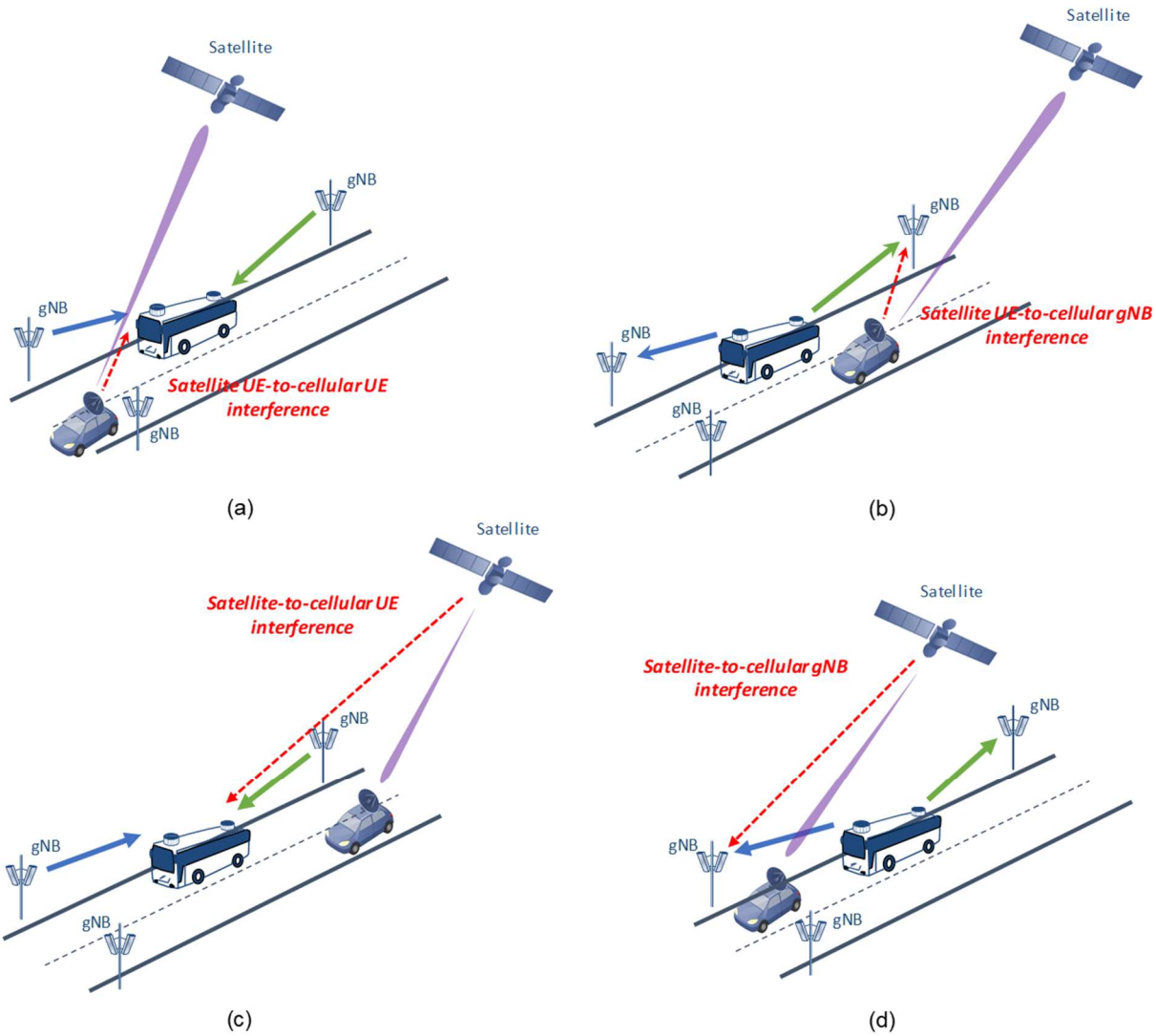

Figure 2-1: Satellite-to-cellular interference scenarios: a) From satellite UE to cellular UE; b) From satellite UE to cellular gNB; c) From satellite to cellular UE; d) From satellite to cellular gNB

The second type of the interference is the cellular-to-satellite interference, i.e. interference from cellular devices to satellite devices. In this case, the interferer can be either a cellular UE, as

shown in Figure 2-2a and Figure 2-2c, or a cellular gNB, as shown in Figure 2-2b and Figure 2-2d. The victim can be either a satellite UE, as shown in Figure 2-2a and Figure 2-2b, or a satellite itself, as shown in Figure 2-2c and Figure 2-2d. Similar to the above satellite-to-cellular interference counterpart, there are four specific scenarios regarding the interference from the cellular link to the satellite link:

- Interference from cellular UE to satellite UE as depicted in Figure 2-2a. This scenario occurs when the satellite link operates in the downlink direction while the cellular link operates in the uplink direction. A significant interference impact is expected due to the short distance of the interference link.
- Interference from cellular gNB to satellite UE as depicted in Figure 2-2b. This scenario occurs when both the satellite and cellular links operate in the downlink directions. A significant interference impact is expected due to short distance between the interferer and the victim.
- Interference from cellular UE to satellite as depicted in Figure 2-2c. This scenario occurs when both the satellite and cellular links operates in the uplink directions. A less significant interference impact is expected due to the long distance of the interference link and the lower transmit power of the cellular UE.
- Interference from cellular gNB to satellite as depicted in Figure 2-2d. This scenario occurs when the satellite link operates in the uplink direction while the cellular link operates in the downlink direction. Due to very long interference link distance and the relatively weak transmit power of the cellular gNB, the interference is expected to be much less significant.

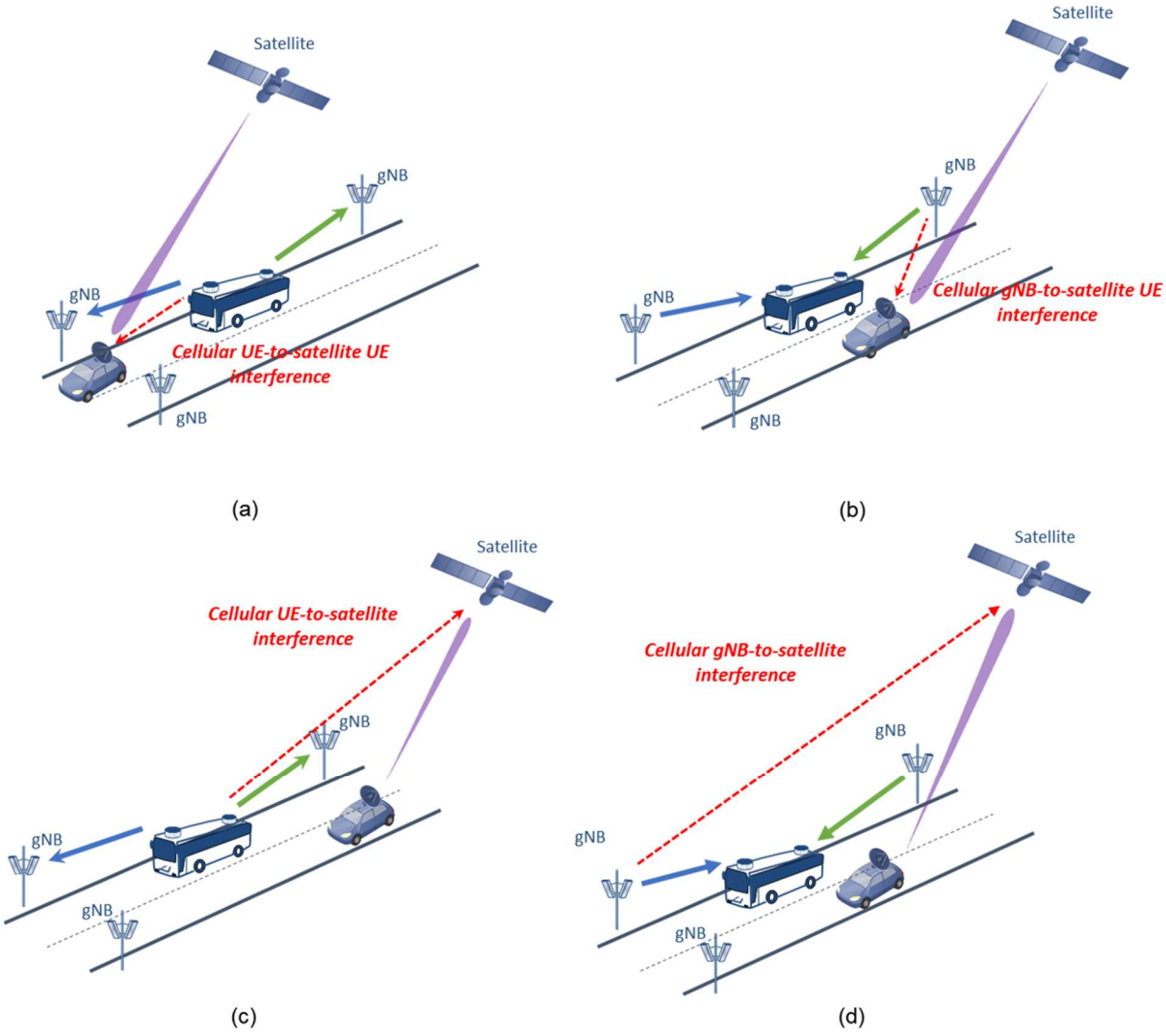

Figure 2-2: Cellular-to-satellite interference scenarios: a) From cellular UE to satellite UE; b) From cellular gNB to satellite UE; c) From cellular UE to satellite; d) From cellular gNB to satellite

Figure 2-3 illustrates the spectrum sharing model consisting of a satellite and a terrestrial system, in which the satellite Earth station receives the desired signal from the satellite while being interfered by BSs.

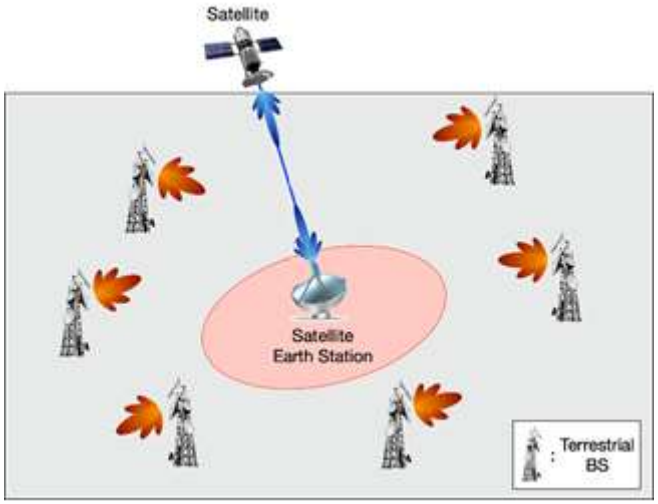

Figure 2-3: Cellular-to-satellite Earth station interference scenario

2.2 Co-channel and adjacent channel interference

The interference situation can be categorized into co-channel interference and adjacent interference depending on the frequency location and bandwidth of each system, as shown in Figure 2-4.

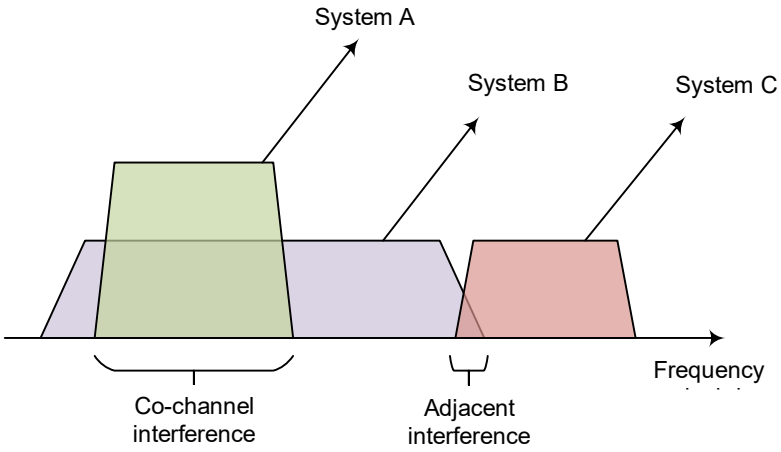

Figure 2-4: Co-channel interference and adjacent interference

Co-channel interference occurs in a situation where the different systems occupy the same portion of the spectrum. In a co-channel interference scenario, the signal reception within the overlapped spectrum is possibly deteriorated at both systems. This kind of interference is most of the time caused by undesirable sidelobes of the transmit or receive antennas. For example, co-channel interference from the terrestrial network onto the satellite system – Figure 2-2 d) – may be caused by undesired sidelobes of transmit gNB antennas, like illustrated in Figure 2-5 left; and interference from the satellite network onto the cellular system – Figure 2-1 d) – may be caused by undesired sidelobes of receive gNB antennas, like illustrated in Figure 2-5 right.

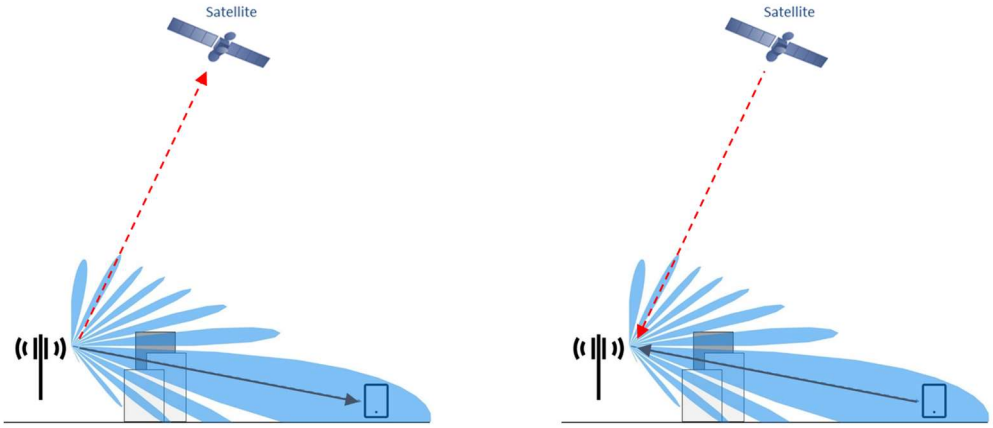

Figure 2-5: Illustration of interference due to undesirable side lobes of cellular antennas, [25]. Left: case of Figure 2-2 d); right: case of Figure 2-1 d).

Co-channel interference may also be caused by a too low separation distance between the receiver and the interfering system. This may be the case for example in Figure 2-2 a) and b) where the satellite UE is too close to the cellular receiver, i.e. within the interfering main beam (see also Figure 4-3).

Adjacent interference occurs in a situation where the spectrum of the different systems does not overlap but are located next to each other. The spectrum near the adjacent part will be affected by the adjacent interference. Hence, the smaller the guard band between both systems, the higher the spectral efficiency.

- This kind of interference may occur when the satellite system shares the bandwidth with the terrestrial system in a coordinated way, i.e. spectrum holes are elaborated in the satellite band so that the terrestrial system benefits from these frequency resources. The width of the holes and their location may be decided by a resource management system, based on several elements like the required Quality of Service (QoS) of terrestrial and satellite users for example.
- A similar situation may also be found in cognitive systems, where the terrestrial system opportunely takes advantage of portions of the band that are not used at a given time by the satellite system.
- Carrier Aggregation (CA) may also be the source of adjacent channel interference, e.g. the spectrum between carriers may be used by another system, like shown in Figure 2-6.

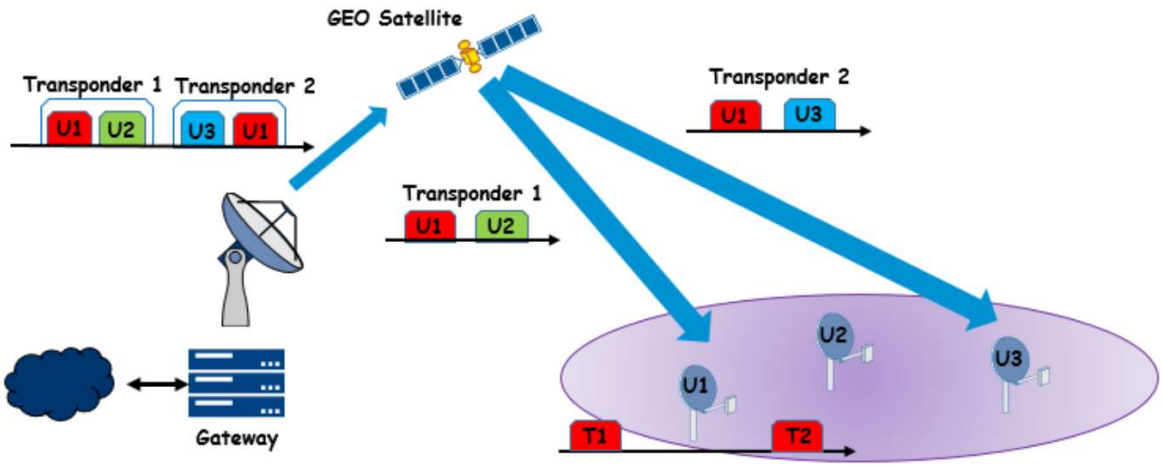

Figure 2-6: Carrier Aggregation in GEO Fixed Satellite Service (FSS) forward link, [28]

Emissions in the adjacent bands can be reduced or nulled thanks to the use of analogue filtering at the output of the RF chain. Nonetheless, in all the situations described above, the multiplicity of the bandwidths would require multiple filters, which is not feasible in practice.

3 Common interference metrics and assumptions

The following list shall give an overview about commonly used metrics in the context of interference analyses in general:

- **Signal-to-Noise Ratio (SNR or S/N):** the ratio between the desired signal power and the noise power.
- **Carrier-to-Noise Ratio (CNR or C/R):** the same as the SNR of a modulated signal before demodulation. Practically, for CNR the power of the desired signal is measured on the useful band whereas for SNR it is measured on the whole band.
- **Signal-to-Interference-and-Noise Ratio (SINR):** the ratio between the desired signal power and the interference plus noise power.
- **Carrier-to-Noise-and-Interference Ratio (CNIR):** the same as the SINR of a modulated signal before demodulation.
- **Signal-to-Interference Ratio (SIR or S/I):** the ratio between the desired signal power and the interference power.
- **Carrier-to-Interference Ratio (CIR or C/I):** the same as the SIR of a modulated signal before demodulation.
- **Geometry Factor:** The geometry factor (GF) is the lower bound for the instantaneous SINR. It does not consider the effects of fast-fading and possible gains of scheduling in the frequency domain. It is defined as the average power ratio of the serving node to the average power of all interfering nodes plus noise.
- **Outage probability:** The probability that Signal to Noise Ratio (SNR) (for interference-free case) or Signal to Interference plus Noise Ratio (SINR) (for interference-prone case) is less than a predefined threshold. An outage event can be interpreted as a communication not satisfying a specific QoS due to a degraded received signal quality [9].

Currently assumed performance requirements for satellite access based on ongoing discussions in 3GPP's Service and System Aspects (SA) working group 1 (SA1) are shown in Table 3-1. These requirements shall give an idea on the expected performance of a satellite access based 5G NR system. Five Scenarios are considered, i.e. pedestrian, vehicular, airborne, stationary and stationary IoT. Noticeable are the high data rates for vehicular, airborne and stationary scenarios, which may be explained by the highly directive antennas that are envisaged for these cases. Interesting for interference analyses is probably the anticipated user densities as well as the activity factors.

Table 3-1: Performance requirements for satellite access, [26]

Scenario	Experienced data rate (DL)	Experienced data rate (UL) (note 1)	Area traffic capacity (DL)	Area traffic capacity (UL)	Overall user density	Activity factor	UE speed	UE type
Pedestrian (note 2)	2 Mbps	250 kbps	3 Mbps/km^2	375 kbps/km^2	100/km^2	1.5%	Pedestrians	Handheld
Vehicular connectivity	50 Mbps	25 Mbps	TBD	TBD	TBD	50%	Up to 250 km/h	Vehicle mounted
Airplanes connectivity (note 3)	360 Mbps	180 Mbps	TBD	TBD	TBD	N/A	Up to 1000 km/h	Airplane mounted
Stationary (note 4)	50 Mbps	25 Mbps	50 Mbps /km^2	25 Mbps /km^2	20/km^2	N/A	Stationary	Building mounted
IoT connectivity	2 kbps	10 kbps	8 kbps/km^2	40 kbps/km^2	400/km^2	1%	Stationary	IoT

Note 1: Area capacity is averaged over a satellite beam.
Note 2: Data rates based on extreme long-range coverage in low density areas
Note 3: Assumption is 120 users per plane and 20% activity factor per user
Note 4: Assumption is 5 users per building and 20% activity factor per user

4 Co-channel interference analysis

The co-channel interference will be analysed in the following subsections by using different approaches. The first approach analyses the outage probability due to interference from BSs onto satellite UEs. A stochastic geometry-based approach to analyse the interference from BSs onto the satellite Earth station follows. Based on the channel models that were developed in the beginning of the project, the last two subsections present the simulations based on the QuaD-RiGa model and the ray-tracing model, respectively.

4.1 Outage probability analysis

The interference scenario depicted in Figure 2-2b is considered in the following. The satellite UE is deployed on a car driving on a road. The desired signal is the satellite downlink signal from the satellite and the interference is the terrestrial downlink signal from the gNB.

Directional beamforming is assumed for both, satellite and terrestrial transmitter-receiver pairs, where a beam is formed with a directivity gain G and a beamwidth BW in an arbitrary 3D direction at each transceiver. However, the specific directivity gain and beamwidth values are different between satellite and terrestrial systems, namely G_{terr} and BW_{terr} for terrestrial gNB/UE and G_{sat} and BW_{sat} for satellite UE, respectively.

As a beam pattern model, a spatial filtering in form of a rectangular mask as defined in the 3GPP 5G channel model is employed [1]. Assuming a boresight direction of $\phi = 0°$, the antenna beam pattern is given by

$$F(\phi, BW) = \begin{cases} G, & |\phi| \leq BW/2 \\ 0, & \text{otherwise.} \end{cases} \tag{4-1}$$

The above rectangular mask is depicted in Figure 4-1.

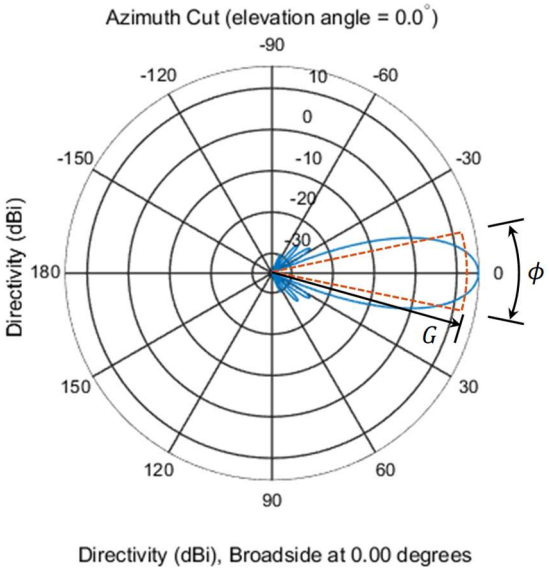

Figure 4-1: Actual beam pattern (blue solid line) and its approximated model based on the rectangular mask model (red dashed line)

For large-scale fading, a standard path loss model is used with a path loss exponent $\alpha > 2$. The channel gains due to small-scale fading follow Nakagami-m fading, which can characterize the multi-path channel having both Line of Sight (LOS) and Non LOS (NLOS) components. Rayleigh fading ($m = 1$) and AWGN ($m \to \infty$) are the two extreme cases. By carefully selecting the m

value, the fading characteristics of both satellite and terrestrial channels can be well characterized while keeping the analytical tractability. The corresponding channel power gain follows a Gamma distribution with the probability density function (PDF) [6]:

$$f_x(x) = \frac{m^m}{\Gamma(m)} x^{m-1} e^{-mx}. \quad (4\text{-}2)$$

The satellite and terrestrial gNB are assumed to transmit with a constant power P_{sat} and P_{terr}, respectively [7], [8].

4.1.1 Interference condition

Considering very high carrier frequencies, which is the case for mmWave bands, it is assumed that interference is effective if and only if there is a LOS link between the interfering transmitter and the interfered receiver and if their transmit and receive beams are aligned with each other, i.e., the interfering transmitter is located within the beamwidth of the receive beam and the interfered receiver is located within the beamwidth of the transmit beam.

Figure 4-2 shows the interference situation of a terrestrial gNB interferer and a satellite UE victim in top view. Assuming a GEO satellite, the satellite UE's receive beam always points to the satellite in the horizontal plane. The terrestrial gNB's transmit beam on the other hand points to a random direction in the horizontal plane. Hence, the satellite UE is only affected by the interferer that is located within the beamwidth of its receive beam and also points its transmit beam towards the satellite UE in the horizontal plane.

Considering the above-mentioned factors, the probability that the satellite UE experiences interference from the terrestrial gNB in the horizontal domain is given by:

$$\text{Prob}_{\text{int},h} = \frac{BW_{\text{terr}}}{360°} \cdot \frac{BW_{\text{sat}}}{360°} \quad (4\text{-}3)$$

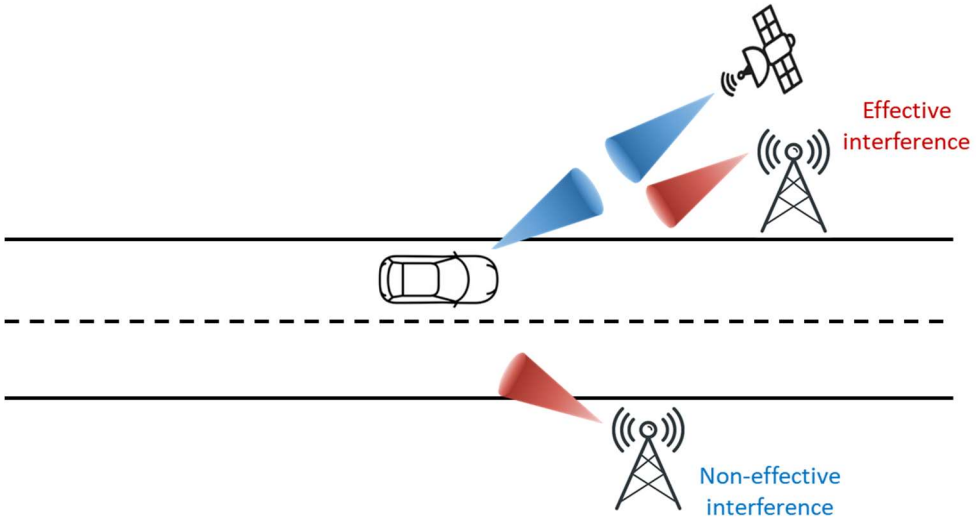

Figure 4-2: Terrestrial-to-satellite interference situation (Top view)

Figure 4-3 shows the interference situation of a terrestrial gNB interferer and a satellite UE victim in side view. A car, equipped with the satellite UE, is assumed to be moving on a road. The elevation angle of the satellite from the car's perspective is almost constant, due to the very large distance between the car and the GEO satellite and the relatively short distance covered by the car. Thus, the vertical direction of the receive beam of the satellite UE is always the same

regardless of the location of the car. On the other side, the terrestrial gNBs are fixed and point to a specific vertical direction. Hence, as the car moves, the satellite UE can be affected by the interference within a specific region (between l_0 and l_1 in Figure 4-3) given that the interference condition in the horizontal domain is met.

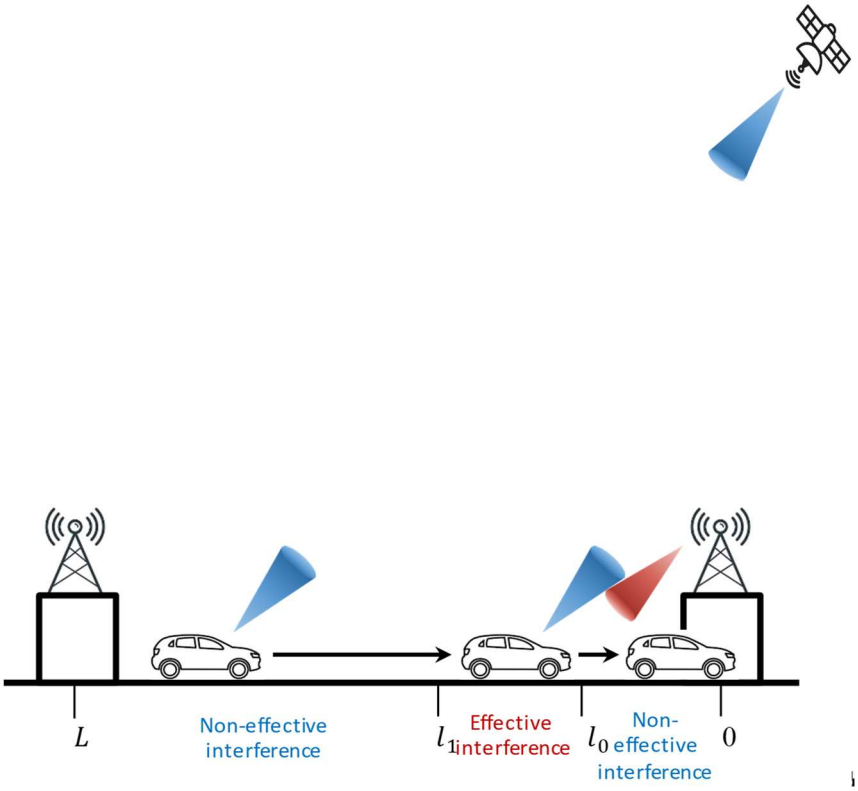

Figure 4-3: Terrestrial-to-satellite interference situation (Side view)

The values of l_0 and l_1 depend on the tilt angle θ_{tilt} of the terrestrial gNB, the elevation angle θ_{elev} of the satellite UE, and the height difference Δ between the terrestrial gNB and satellite UE, as given by:

$$l_0 = \frac{\Delta}{\tan\left(\theta_{\text{tilt}} + \frac{BW_{\text{terr}}}{2}\right)} \tag{4-4}$$

$$l_1 = \frac{\Delta}{\tan\left(\theta_{\text{elev}} - \frac{BW_{\text{sat}}}{2}\right)} \tag{4-5}$$

Then, the probability that the satellite UE located at l experiences interference from the terrestrial gNB in the vertical domain is given by

$$\text{Prob}_{\text{int},v} = \Pr\{l_0 \le l < l_1\}. \tag{4-6}$$

4.1.2 Outage probability

Considering the above interference condition, the outage probability can be defined as

$$\text{Prob}_{\text{out}} = \text{E}_l[\Pr\{SNR \le T\}\Pr\{l < l_0, l \ge l_1\} + \Pr\{SINR \le T\}\Pr\{l_0 \le l < l_1\}], \tag{4-7}$$

where T is the threshold for SNR or SINR. Meanwhile, the SNR and the SINR can be expressed as

$$SNR = \frac{hr^{-\alpha_{\text{sat}}} G_{\text{sat}} P_{\text{sat}}}{N_0}, \tag{4-8}$$

$$SINR = \frac{hr^{-\alpha_{\text{sat}}} G_{\text{sat}} P_{\text{sat}}}{gl^{-\alpha_{\text{terr}}} G_{\text{terr}} P_{\text{terr}} + N_0}, \tag{4-9}$$

where h and g are channel power gains for the desired (i.e., satellite) and interference (i.e., terrestrial) links, respectively. N_0 is the noise power density. r is the distance between the satellite and the satellite UE, which can be calculated according to [3] with:

$$r = \sqrt{R_E^2 \sin^2 \theta_{\text{elev}} + h_0^2 + 2h_0 R_E} - R_E \sin \theta_{\text{elev}}. \tag{4-10}$$

where R_E denotes the radius of the Earth and h_0 denotes the altitude of the satellite.

The Nakagami fading parameters are assumed to be m for the terrestrial link and n for the satellite links, respectively. Then, the individual outage probability for the non-effective interference case in (4-7) yields

$$\begin{aligned} \Pr\{SNR \le T\} &= \Pr\left\{h \le \frac{TN_0 r^{\alpha_{\text{sat}}}}{G_{\text{sat}} P_{\text{sat}}}\right\} \\ &= \frac{\gamma\left(n, \frac{nTN_0 r^{\alpha_{\text{sat}}}}{G_{\text{sat}} P_{\text{sat}}}\right)}{\Gamma(n)}, \end{aligned} \tag{4-11}$$

where $\gamma(\cdot,\cdot)$ denotes the incomplete Gamma function and $\Gamma(\cdot)$ denotes the Gamma function, respectively. Meanwhile, assuming interference-limited scenario (i.e., $gl^{-\alpha_{\text{terr}}} G_{\text{terr}} P_{\text{terr}} \gg N_0$), the individual outage probability for the effective interference case in (4-7) can be rewritten as

$$\Pr\{SINR \le T\} = \Pr\left\{\frac{g}{h} \ge \frac{l^{\alpha_{\text{terr}}} G_{\text{sat}} P_{\text{sat}}}{Tr^{\alpha_{\text{sat}}} G_{\text{terr}} P_{\text{terr}}}\right\}. \tag{4-12}$$

After substitution of $z = g/h$, employing the property of the function of two random variables [10] and then using (3.326) of [11], the PDF yields

$$\begin{aligned} f_z(z) &= \int_0^\infty y f_{gh}(yz, y) dy \\ &= \frac{m^m n^n z^{m-1}}{\Gamma(m)\Gamma(n)} \int_0^\infty y^{m+n-1} e^{-(mz+n)y} dy \\ &= \frac{\Gamma(m+n) m^m}{\Gamma(m)\Gamma(n) n^m} \frac{z^{m-1}}{\left(1 + \frac{m}{n} z\right)^{m+n}}. \end{aligned} \tag{4-13}$$

Then, (4-12) can be rewritten as

$$\begin{aligned} \Pr\{SINR \le T\} &= \Pr\left\{z \ge \frac{l^{\alpha_{\text{terr}}} G_{\text{sat}} P_{\text{sat}}}{Tr^{\alpha_{\text{sat}}} G_{\text{terr}} P_{\text{terr}}}\right\} \\ &= \frac{\Gamma(m+n) m^m}{\Gamma(m)\Gamma(n) n^m} \int_{\frac{l^{\alpha_{\text{terr}}} G_{\text{sat}} P_{\text{sat}}}{Tr^{\alpha_{\text{sat}}} G_{\text{terr}} P_{\text{terr}}}}^\infty \frac{z^{m-1}}{\left(1 + \frac{m}{n} z\right)^{m+n}} dz. \end{aligned} \tag{4-14}$$

The integration can be solved with the help of (3.194.2) in [11]:

$$\Pr\{SINR \le T\} = \frac{\Gamma(m+n)n^{n-1}}{\Gamma(m)\Gamma(n)m^n}\left(\frac{Tr^{\alpha_{\text{sat}}}G_{\text{terr}}P_{\text{terr}}}{l^{\alpha_{\text{terr}}}G_{\text{sat}}P_{\text{sat}}}\right) \times {}_2F_1\left(m+n, n; 1+n; -\frac{n}{m}\frac{Tr^{\alpha_{\text{sat}}}G_{\text{terr}}P_{\text{terr}}}{l^{\alpha_{\text{terr}}}G_{\text{sat}}P_{\text{sat}}}\right), \tag{4-15}$$

where ${}_2F_1(\cdot,\cdot;\cdot;\cdot)$ is the hypergeometric function [11].

Assuming l is uniformly distributed between 0 and L, the outage probability in (4-7) can be expressed as

$$\text{Prob}_{\text{out}} = \underbrace{\Pr\{SINR \le T\}\left(\frac{l_0 + L - l_1}{L}\right)}_{\text{Prob}_{\text{out},0}} + \underbrace{\text{Prob}_{\text{int},h}\int_{l_0}^{l_1}\Pr\{SINR \le T\}dl.}_{\text{Prob}_{\text{out},1}} \tag{4-16}$$

The interference-free part of the outage probability $\text{Prob}_{\text{out},0}$ can be obtained using (4-11):

$$\text{Prob}_{\text{out},0} = \left(\frac{l_0 + L - l_1}{L}\right)\frac{\gamma\left(n, \frac{nTN_0r^{\alpha_{\text{sat}}}}{G_{\text{sat}}P_{\text{sat}}}\right)}{\Gamma(n)}. \tag{4-17}$$

The interference-prone part of the outage probability $\text{Prob}_{\text{out},1}$ is given by

$$\text{Prob}_{\text{out},1} = \text{Prob}_{\text{int},h}\frac{\Gamma(m+n)n^{n-1}}{\Gamma(m)\Gamma(n)m^n}\left(\frac{Tr^{\alpha_{\text{sat}}}G_{\text{terr}}P_{\text{terr}}}{G_{\text{sat}}P_{\text{sat}}}\right) \times \int_{l_0}^{l_1} l^{-\alpha_{\text{terr}}}\,{}_2F_1\left(m+n, n; 1+n; -\frac{n}{m}\frac{Tr^{\alpha_{\text{sat}}}G_{\text{terr}}P_{\text{terr}}}{l^{\alpha_{\text{terr}}}G_{\text{sat}}P_{\text{sat}}}\right)dl. \tag{4-18}$$

Using the identity of $\int x^{\beta-1}\,{}_pF_q\left((a_p);(b_q);x\right)dx = \frac{x^\beta}{\beta}\,{}_{p+1}F_{q+1}\left((a_p),\beta;(b_q),\beta+1;x\right)$ in [12], the closed-form expression of (4-18) can be obtained as

$$\begin{aligned}\text{Prob}_{\text{out},1} = \text{Prob}_{\text{int},h}&\frac{\Gamma(m+n)n^{n-1}}{\Gamma(m)\Gamma(n)m^n}\frac{\left(\frac{Tr^{\alpha_{\text{sat}}}G_{\text{terr}}P_{\text{terr}}}{G_{\text{sat}}P_{\text{sat}}}\right)}{1-\alpha_{\text{terr}}n} \\ \times\Bigg[l_1^{1-\alpha_{\text{terr}}}\,{}_3F_2&\left(m+n, n-\frac{1-\alpha_{\text{terr}}n}{\alpha_{\text{terr}}}; 1+n, 1-\frac{1-\alpha_{\text{terr}}n}{\alpha_{\text{terr}}}; -\frac{n}{m}\frac{Tr^{\alpha_{\text{sat}}}G_{\text{terr}}P_{\text{terr}}}{G_{\text{sat}}P_{\text{sat}}}l_1^{-\alpha_{\text{terr}}}\right) \\ -\,l_0^{1-\alpha_{\text{terr}}}\,{}_3F_2&\left(m+n, n-\frac{1-\alpha_{\text{terr}}n}{\alpha_{\text{terr}}}; 1+n, 1-\frac{1-\alpha_{\text{terr}}n}{\alpha_{\text{terr}}}; -\frac{n}{m}\frac{Tr^{\alpha_{\text{sat}}}G_{\text{terr}}P_{\text{terr}}}{G_{\text{sat}}P_{\text{sat}}}l_0^{-\alpha_{\text{terr}}}\right)\Bigg].\end{aligned} \tag{4-19}$$

4.1.3 Results

The analysis done for finding outage probability of shared spectrum access between satellite and terrestrial networks is verified by simulation. For the analysis and simulation, the following parameters are assumed:

- Altitude of GEO satellite: $h_0 = 35786$ km
- Earth radius: $R_E = 6371$ km
- Elevation angle: $\theta_{\text{elev}} = 45°$
- Inter-site distance: $L = 0.1$ km

- height difference between terrestrial gNB and satellite UE: $\Delta = 23.5\ \mathrm{m}$
- Tilt angle: $\theta_{\mathrm{tilt}} = 20°$
- Path-loss exponent: $\alpha_{\mathrm{sat}} = 2.1$, $\alpha_{\mathrm{terr}} = 3$
- K-factor: $K_{\mathrm{sat}} = 10\ \mathrm{dB}$, $K_{\mathrm{terr}} = 5\ \mathrm{dB}$
- Transmit power: $P_{\mathrm{sat}} = 20\ \mathrm{W}$, $P_{\mathrm{terr}} = 0.1\ \mathrm{W}$
- Beamforming gain: $G_{\mathrm{sat-t}} = 58.5\ \mathrm{dBi}$, $G_{\mathrm{sat-ue}} = 20\ \mathrm{dBi}$, $G_{\mathrm{terr}} = 20\ \mathrm{dBi}$
- Beamwidth: $BW = 30°$

The analysis and simulation results are depicted in Figure 4-4. For the simulation, 1,000,000 iterations are carried out. It shows that the analysis and simulation results coincide each other. It is also observed that the existence of the interference yields higher outage probability especially in low SNR/SIR threshold region.

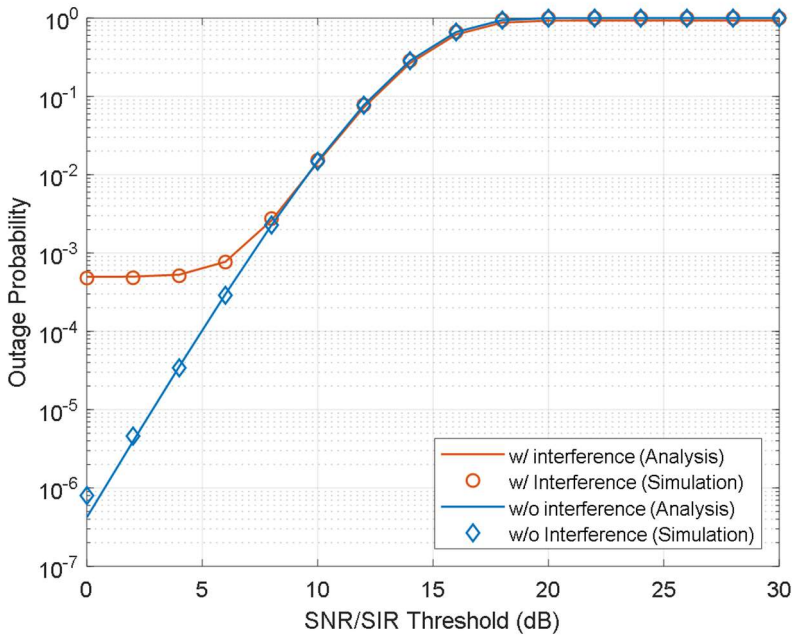

Figure 4-4: Outage probability vs. SNR/SIR threshold

4.2 Stochastic geometry-based analysis

Stochastic geometry is a well-known study on the random spatial patterns in mathematics [13]. Since the stochastic geometry can represent the geometric correlation among randomly generated points in spatial domain, it has been widely used for analysing the performance of wireless communication networks by reflecting random location of base stations (BSs) and user equipment (UEs), cell sectorization, antenna model, directional antennas, multiple antennas, heterogeneous cell-layout, path-loss characteristics, multi-user scheduling, shadowing effect, mobility, cooperative operation among BSs, etc [14], [15], [16], [17], [18], [19], [20], [21].

In addition, several studies on mutual interference between the terrestrial wireless network and the satellite system have been conducted, but they are based on deterministic geometry of BSs or UEs [22], [23]. This section provides the interference analysis framework based on stochastic geometry. The interference of interest is the one from the BSs to the satellite Earth station. Through the stochastic geometry-based analysis, statistical properties of mutual interference

between the satellite system and the terrestrial 5G systems can be analysed.

4.2.1 Interference analysis

In general, the stochastic geometry is used to analyse various performances of wireless network such as interference characteristics, throughput, and coverage probability, etc. Recently, various communication scenarios have been investigated based on the stochastic geometry in 5G networks [14], [15], [16], [17], [18], [19], [20], [21].

1. **Ultra-dense networks**

   In heterogeneous ultra-dense networks, inter-cell interference is a major technical challenge. In the heterogeneous ultra-dense networks, a large number of BSs are expected to be deployed in a certain area and they have dissimilar characteristics in terms of deployment density, transmit power, antenna gain, multiple access technique, etc. It has been shown that the locations of heterogeneous BSs are well modelled with the stochastic geometry, and many attempts have been made for modelling, analysing, and simulating heterogeneous ultra-dense networks with stochastic geometry in literature [14].

2. **mm-Wave bands**

   In many countries, mm-Wave bands are used for hot spots or very high capacity mobile services in 5G. The channel characteristics of mm-Wave frequencies are significantly different from lower frequencies at around 700 MHz or around 3.5 GHz, although they are highly correlated in terms of their LOS/NLOS condition. In addition, the LOS and NLOS characteristics severely depend on distance and obstacles between the communication nodes. In general, massive multiple input multiple output (MIMO) and hybrid beamforming techniques are exploited to improve signal strength and mitigate interference in mm-Wave bands. By considering the LOS/NLOS condition and beamforming techniques, the signal-to-interference-plus-noise (SINR) has been analysed based on the stochastic geometry [15]. In particular, the stochastic geometry-based coverage probability analysis has been evaluated by considering a realistic mm-Wave channel model, practical antenna radiation patterns, beamforming misalignment effect, etc. [16].

3. **Directional antennas & hybrid beamforming techniques**

   In 5G systems, both BS and UE are equipped with multiple antennas, and transmit and receive beamforming techniques are exploited. In particular, planar or linear antenna arrays are expected to be implemented at the BS and the UE, respectively, especially for mm-Wave bands. Therefore, 5G systems can be regarded as directional wireless networks where both transmitter and receiver operate with directional antennas (or equivalently directional beamforming techniques via multiple antennas). The directional antennas help increase signal strength and reduce interference at the same time. The directivity (or spatial domain selectivity) is defined either in two-dimensional or three-dimensional space based on the geometry of the array antenna and the radiation patterns of the individual antenna elements. The stochastic geometry with a simplified two-dimensional antenna gain pattern was also used for modelling and analysing the performance of such a directional wireless network, where the effect of beam misdirection or misalignment on performance including coverage and throughput was investigated as well [17].

4. **Satellite & non-terrestrial networks**

   To accommodate the explosively increasing number of wireless devices and data traffic, 5G system is no longer limited to terrestrial networks and thus the integration between the conventional terrestrial cellular networks and non-terrestrial communication segments are being actively studied. For an important example, communication satellites can provide global coverage. In addition, they can connect remote communication nodes including airborne and seaborne platforms. Future Medium Earth Orbit (MEO)

and LEO satellites are expected to provide improved communication capabilities with higher frequency reuse. Manned/unmanned aerial vehicles and drones will improve the terrestrial 5G network in terms of coverage, throughput, flexibility, etc. Recently, the stochastic geometry-based framework was also applied for analysing the performance of non-terrestrial networks [14], [18], [19], [20]. The conventional two-dimensional stochastic geometry framework can only be used if the communication nodes are located at a relatively low altitude, ranging from a few meters to tens of meters. However, two-dimensional stochastic geometry cannot be directly applied to the case where altitudes of aerial communication nodes range from several kilometres to more than 30,000 km. In this case, three-dimensional stochastic geometry models are required. Furthermore, the high altitude of the non-terrestrial communication nodes significantly affects the LOS probability of communication links and with that the corresponding interference analysis.

4.2.2 Network model

Let us consider a spectrum sharing scenario between the terrestrial 5G system and the satellite communication system. In the following, we focus on the downlink case for both systems and only consider the interference from the terrestrial 5G system (i.e., BSs) to a certain Satellite Earth Station (SES), as described in Figure 2-3. The interference from a corresponding satellite to the BSs indeed exists, but it can be neglected since the received signal power from the satellite is low and the antennas of the BSs are down-tilted in general. The stochastic geometry is used to analyse the aggregated interference at the SES. To be specific, the BSs are assumed to be located randomly according to a homogeneous Poisson point process (PPP) with density λ in two-dimensional space (area). Figure 4-5 shows the location of BSs and the cell-boundaries, where λ is equal to 0.3/km^2, 0.5/km^2, and 1.0/km^2, respectively.

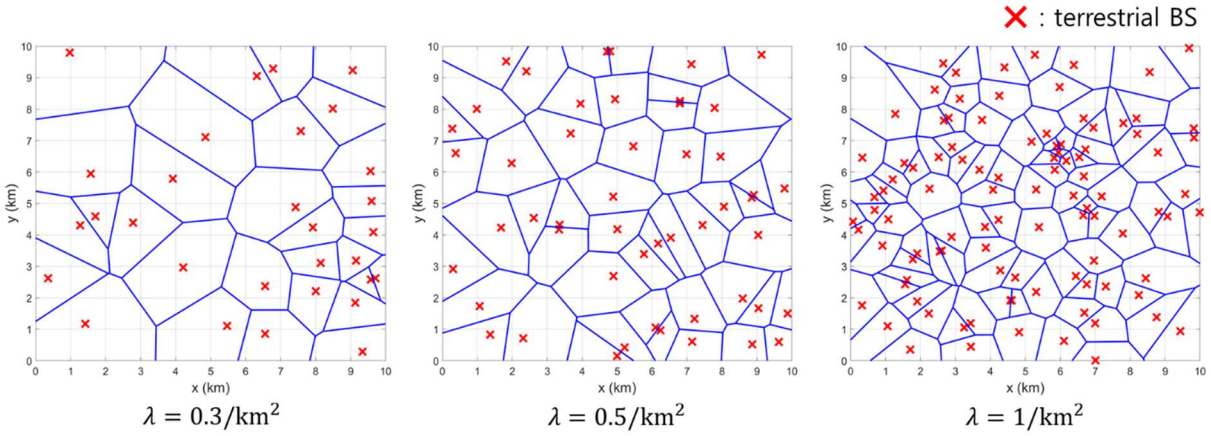

Figure 4-5: Location of BSs and cell-boundaries

The SES is assumed to be located in the center of the two-dimensional area, A_0, and the cellular base stations are distributed according to PPP with the density of λ in the same area. In addition, if we set the circular exclusive zone with radius R_E around the satellite earth station, any BSs is located at least R_E radius away from the satellite earth station. Then, the area of the exclusion zone is given by $A_{\mathrm{E}} = \pi R_{\mathrm{E}}^2$, and the resultant density of the BSs with exclusion zone is given by $\lambda_{\mathrm{E}} = \frac{\lambda A_0}{(A_0 - A_{\mathrm{E}})}$. Figure 4-6 shows the network model consisting of the BSs with exclusion zone and the satellite earth station.

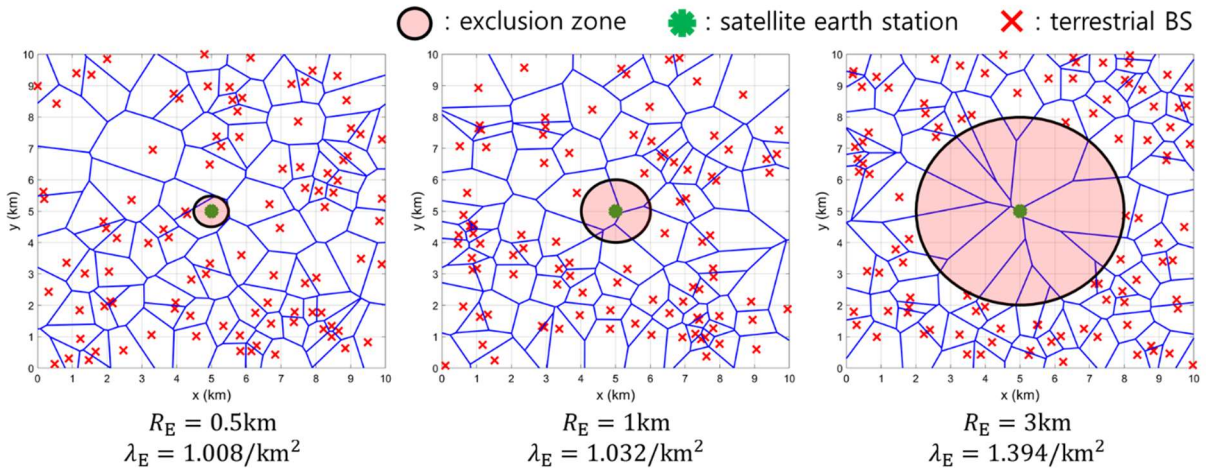

Figure 4-6: Location of the BSs with exclusion zone and the satellite earth station

The height of the BSs is neglected for convenience since it does not significantly affect performance in practice. The BSs are assumed to exploit azimuthal transmit beamforming techniques and thus the directional transmit beam pattern in azimuth angle domain is only considered for analysing the received interference at the satellite earth station. It is assumed that all BSs have the same ideal azimuth (horizontal) beamforming gain within the main-lobe beamwidth ω_C, and its normalized azimuth gain is given as [17]:

$$G_C(\phi) = \begin{cases} g_{1,C} & ,\text{if } |\phi| \le \frac{\omega_C}{2} \\ g_{2,C} & ,\text{otherwise} \end{cases}$$

where $g_{1,C}$ and $g_{2,C}$ denote the gain of the main-lobe and the side-lobe of BSs, respectively, and $\frac{1}{2\pi}\int_{-\pi}^{\pi} G_C(\phi)d\phi = 1$.

$$g_{1,C} = \frac{2\pi - g_{2,C}(2\pi - \omega_C)}{\omega_C}$$

On the other hand, the satellite earth station is typically equipped with a parabolic antenna and the receive antenna gain varies dynamically in three-dimensional space. In this document, however, we assume the receive antenna gain is given by [24]

$$G_S(\phi,\theta) = \begin{cases} g_{1,S} & ,\text{if } |\phi| \le \frac{\omega_S}{2} \ \&\ |\theta| \le \frac{\omega_S}{2} \\ g_{2,S} & ,\text{otherwise} \end{cases}$$

where ω_S denotes the beamwidth of the main-lobe, while $g_{1,S}$ denotes the constant antenna gain of the main-lobe

$$g_{1,S} = \frac{4\pi - g_{2,S}\left(A_{\text{sphere}} - A_{\text{side}}(\omega_S)\right)}{A_{\text{main}}(\omega_S)}$$

and $g_{2,S}$ denotes the constant antenna gain of and side-lobe

$$g_{2,\mathrm{S}} = \frac{P_s}{A_{\mathrm{side}}(\omega_{\mathrm{S}})}$$

Further, A_{sphere} denotes the surface area of a sphere, while $A_{\mathrm{main}}(\omega_S)$ and $A_{\mathrm{side}}(\omega_S)$ denote the radiation area of main-lobe and side-lobe and depend on the beamwidth ω_S.

$$A_{\mathrm{main}}(\omega_{\mathrm{S}}) = \int_{\theta=0}^{\omega_{\mathrm{S}}} \int_{\phi=0}^{\omega_{\mathrm{S}}} \sin\phi \, d\phi d\theta$$

$$A_{\mathrm{side}}(\omega_{\mathrm{S}}) = A_{\mathrm{sphere}} - A_{\mathrm{main}}(\omega_{\mathrm{S}})$$

The transmit antenna gain of the satellite is in general weaker than the receive antenna gain of the satellite earth station due to its large parabolic antenna, nonetheless we assume that the transmit antenna gain of the satellite is the same as the receive antenna gain of the satellite earth station, $G_{\mathrm{S}}(\phi, \theta)$, for convenience. We assume that both, the satellite and the satellite earth station are perfectly aligned with each other.

Now, we introduce the geometric relationship between the terrestrial BS and the satellite earth station in detail to analyse the interference at the satellite earth station from the BSs. Both, the BS and the satellite earth station have highly directional antennas and thus the interference significantly varies according to whether the beams are aligned with each other or not. The orientation of the transmit beamforming at BSs is determined by the location of the cellular UEs in two-dimensional space with the azimuth angle, while the orientation of the receive directional antenna at the satellite earth station is determined by the direction towards the satellite given in azimuth and elevation angle. Therefore, the geometrical relationship between the i-th BS and the satellite earth station is shown as Figure 4-7.

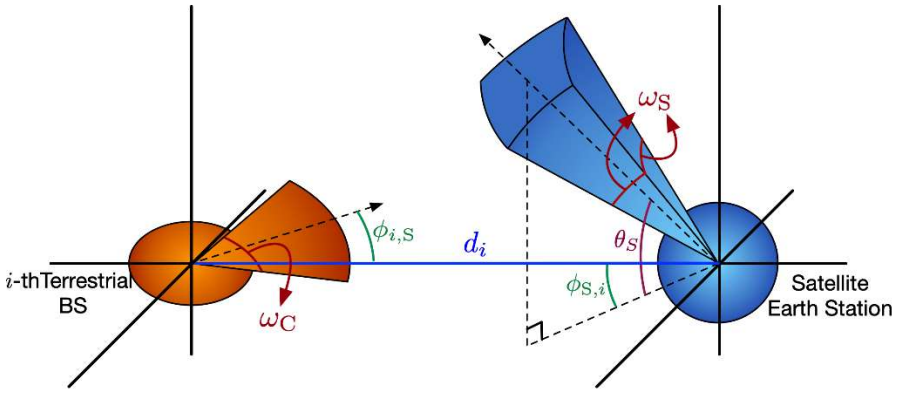

Figure 4-7: Geometry between the BS and the SES

In Figure 4-7, $\phi_{i,\mathrm{S}}$ denotes the angle between the horizontal direction of the i-th BS towards the satellite earth station and the horizontal beam direction of the i-th BS, while $\phi_{\mathrm{S},i}$ denotes the angle between the horizontal direction of the satellite earth station towards the i-th BS and the horizontal beam direction of the satellite earth station. Both $\phi_{i,\mathrm{S}}$ and $\phi_{\mathrm{S},i}$ are assumed to be uniformly distributed over $[-\pi, \pi]$. In addition, θ_{S} denotes the elevation angle of the receive directional antenna at the satellite earth station and it is assumed to be uniformly distributed over $[0, \pi/2\,]$ as well. The distance between the i-th BS and the satellite earth station is given by d_i.

The transmit beamforming gain of the BS is determined by the angle $\phi_{i,\mathrm{S}}$. On the other hand, the receive beamforming gain of the satellite earth station is determined by the azimuth angle $\phi_{\mathrm{S},i}$ as well as the elevation angle θ_{S}. Note that all the interferences from the BSs to the SES

will experience side-lobe antenna gain at the satellite earth station, $g_{2,\mathrm{S}}$, if $\theta_{\mathrm{S}} \geq \frac{\omega_{\mathrm{S}}}{2}$ is satisfied. Thus, the condition of signal reception through the main-lobe antenna gain at the satellite earth station is that the received signal arrives within both the azimuth angle range and the elevation angle range of the main-lobe antenna gain at the same time.

Considering a GEO satellite located at an altitude h_{S} of about 36,000 km, the distance d_{S} between the satellite and the satellite earth station for a given θ_{S} is given by

$$d_{\mathrm{S}} = \frac{36{,}000}{\sin(\theta_{\mathrm{S}})}.$$

Figure 4-8 illustrates the spectrum sharing model consisting of the satellite and terrestrial cellular systems.

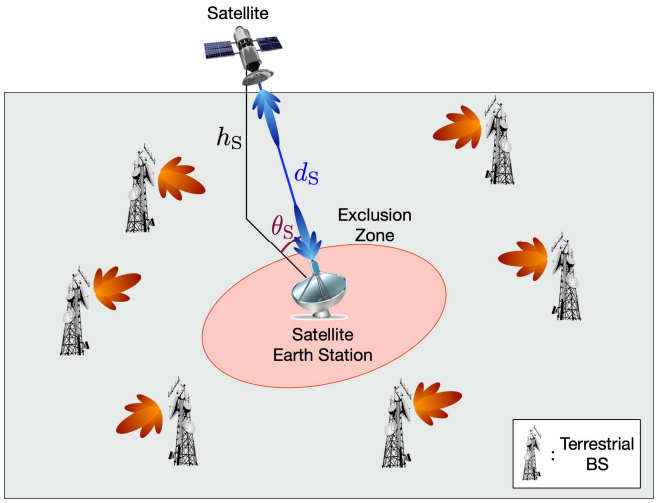

Figure 4-8: Spectrum sharing model between satellite and terrestrial cellular systems

The interference power from the i-th BS to the satellite earth station is given by

$$I_{i,\mathrm{S}} = G_{\mathrm{S}}(\phi_{\mathrm{S},i}, \theta) d_i^{-\alpha} G_{\mathrm{C}}(\phi_{i,\mathrm{S}}) P_{t,\mathrm{C}}$$

where α and $P_{t,\mathrm{C}}$ denote the path-loss exponent and the transmit power of the BS, respectively. The received power of the desired signal of the satellite earth station is given by

$$P_{\mathrm{S}} = G_{\mathrm{S}}(0,0) d_{\mathrm{S}}^{-\alpha} G_{\mathrm{S}}(0,0) P_{t,\mathrm{S}} = g_{1,\mathrm{S}}^2 d_{\mathrm{S}}^{-\alpha} P_{t,\mathrm{S}},$$

where $P_{t,S}$ denotes the transmit power of the satellite. Hence, the aggregated interference from the all BSs at the satellite earth station is given by

$$I_S = \sum_{\forall i} I_{i,\mathrm{S}}$$

and the received signal-to-interference ratio (SIR) is given by

$$\mathrm{SIR} = \frac{P_{\mathrm{S}}}{I_{\mathrm{S}}}.$$

4.2.3 Results

In this section, the simulation results are shown in terms of cumulative density function (CDF) of the aggregated interference and the expected interference at the satellite earth station. The SIR is inversely proportional to the aggregated interference assuming constant satellite transmit power. The parameters used in simulations are summarized in Table 4-1.

Table 4-1: System Parameters in Simulation

Area of 2D ground (A_0)	$10 \times 10\ \mathrm{km}^2$
BS density (λ)	$0.5/\mathrm{km}^2$
Radius of the exclusion zone (R_E)	$1\mathrm{km}$
SES beamwidth (ω_S)	$20°$
BS beamwidth (ω_C)	$60°$
SES elevation angle (θ_S)	$60°$
Satellite transmit power $(P_{t,S})$	20W
BS transmit power $(P_{t,\mathrm{C}})$	5W
SES antenna side-lobe gain $(g_{2,\mathrm{S}})$	0.1
BS antenna side-lobe gain $(g_{2,\mathrm{C}})$	0.1

Figure 4-9 shows the CDF of the aggregated interference at the satellite earth station for different values of θ_S while $\omega_S = 20°$. In the spectrum sharing scenarios, the elevation angle of the satellite earth station is one of the most important factors to affect the interference characteristics. As noted before, the main lobe may be steered directly toward the BSs if the elevation angle of the satellite earth station is less than $\omega_\mathrm{S}/2$. Thus, when $\theta_\mathrm{S} = 60°$ where the elevation angle of the satellite earth station is greater than $\frac{\omega}{2}$, all the interference from the BSs arrives over the side lobe of the SES and the aggregated interference is relatively low. On the other hand, for $\theta_\mathrm{S} = 5°$, the interference from the BSs can be received over the main lobe or the side lobe of the SES according to orientation angles of both, the BSs and the SES, leading to a much larger resultant aggregated interference than in the case if the elevation angle of the satellite earth station is less than $\omega_\mathrm{S}/2$. Figure 4-10 shows the expected interference at the satellite ground station according to the elevation angle. In this figure, the expected interference has a stepped tendency for varying the elevation angle of the SES.

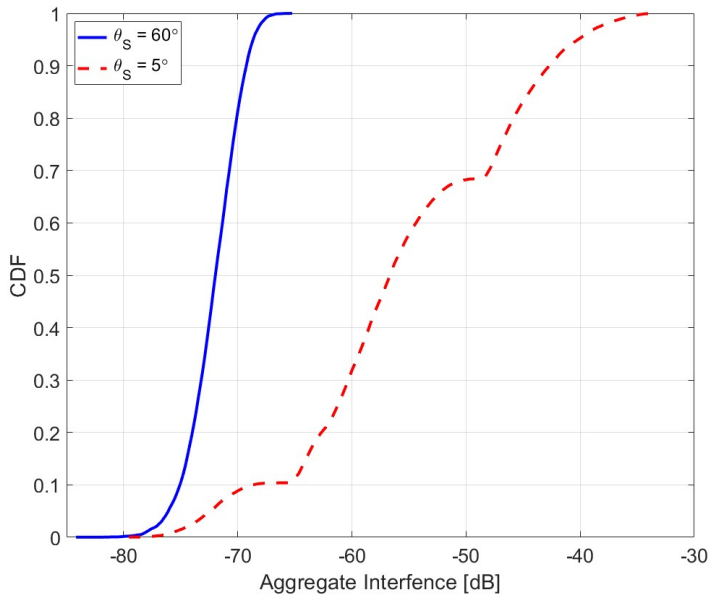

Figure 4-9: CDF of aggregated interference according to θ_S when $\omega_S = 20°$

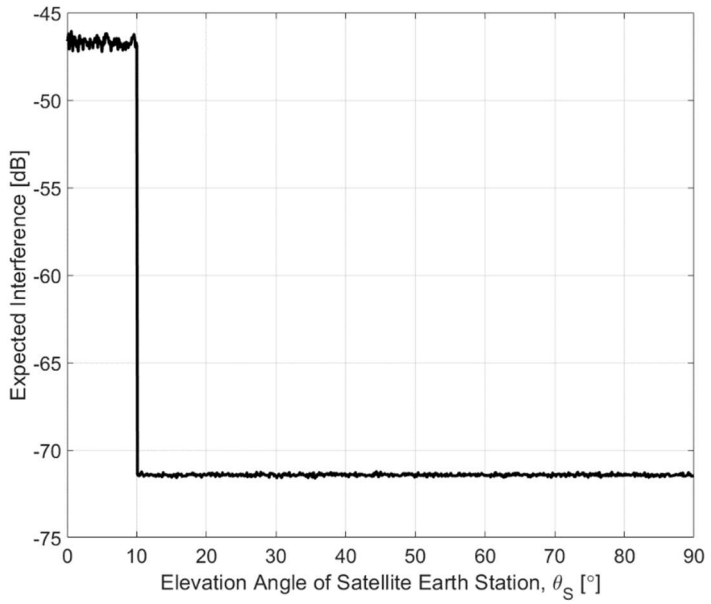

Figure 4-10: Expected interference according to θ_S when $\omega_S = 20°$

Figure 4-11 shows the CDF of the aggregated interference at the satellite earth station according to the radius of exclusion zone R_E. When the original BS density λ is fixed, i.e., $\lambda = 0.5/\mathrm{km}^2$, the adjusted densities λ_E due to exclusion zone become $0.504/\mathrm{km}^2$, $0.516/\mathrm{km}^2$, and $0.572/\mathrm{km}^2$ if $R_E = 500\mathrm{m}$, $1000\mathrm{m}$, and $2000\mathrm{m}$, respectively. As expected, the aggregated interference decreases as the exclusion zone becomes larger. Figure 4-12 shows the expected aggregated interference according to the radius of exclusion zone. The exclusion zone-based interference management can be an effective solution.

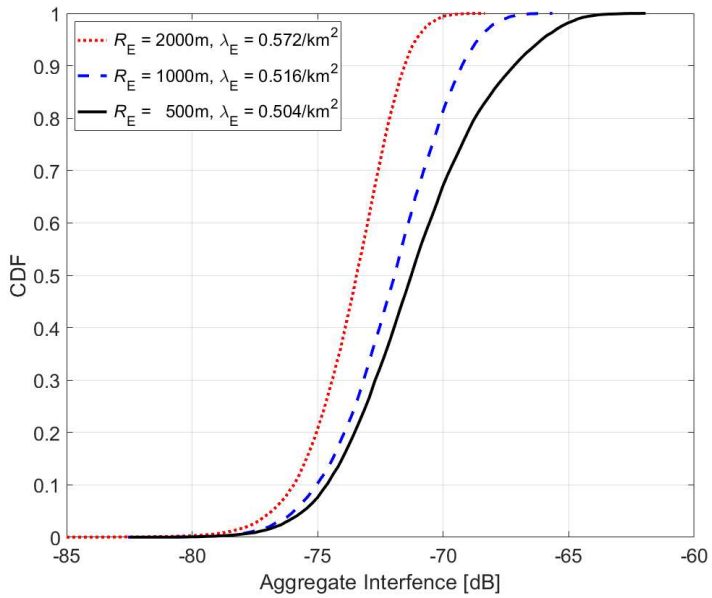

Figure 4-11: CDF of aggregated interference according to R_E

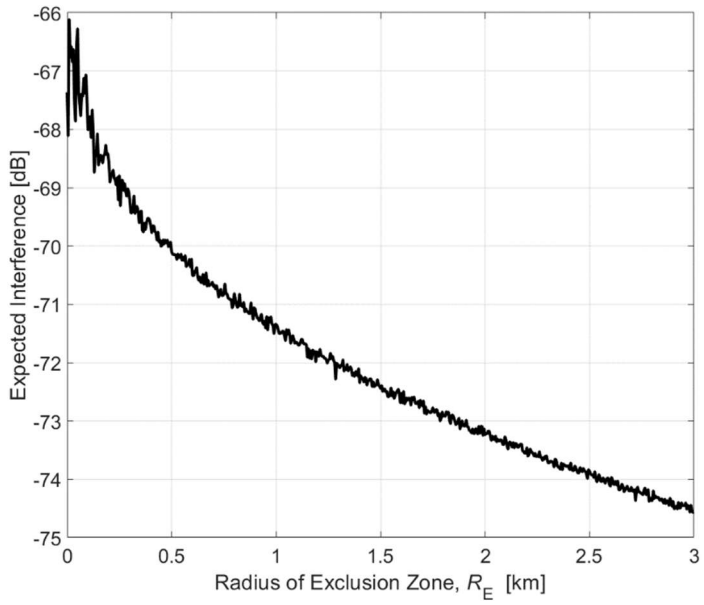

Figure 4-12: Expected interference according to θ_S

Figure 4-13 shows the CDF of aggregated interference at the satellite earth station according to the BS density, i.e., $\lambda = 0.3/\text{km}^2$, $0.5/\text{km}^2$, and $0.7/\text{km}^2$. As expected, the aggregated interference at the satellite earth station increases, as the BS density increases.

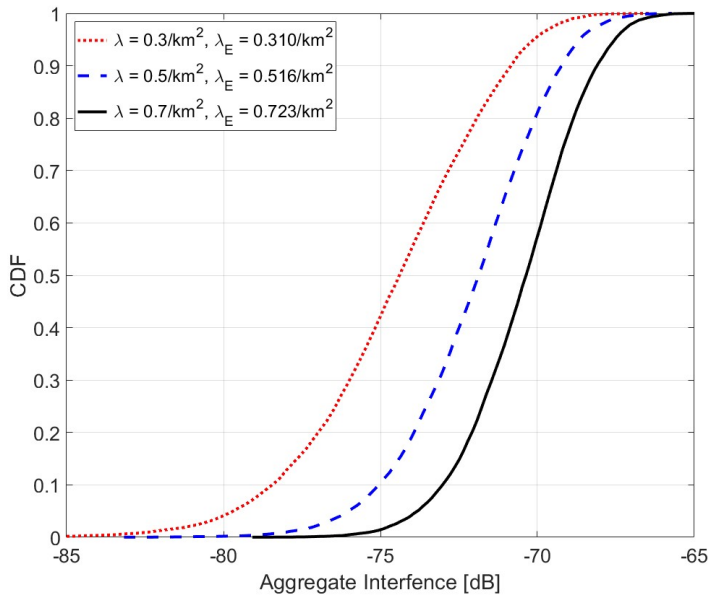

Figure 4-13: CDF of aggregated interference according to λ

Figure 4-14 shows the CDF of the aggregated interference at the satellite earth station according to the BS beamwidth, i.e., $\omega_C = 80°$, $60°$, and $40°$. As ω_C becomes smaller, the variance of the interference at the satellite earth station increases, which implies the interference from the BSs with narrow beam varies dynamically according to whether the interference at the satellite earth station from a certain BS is sent by main lobe beam or by side lobe beam.

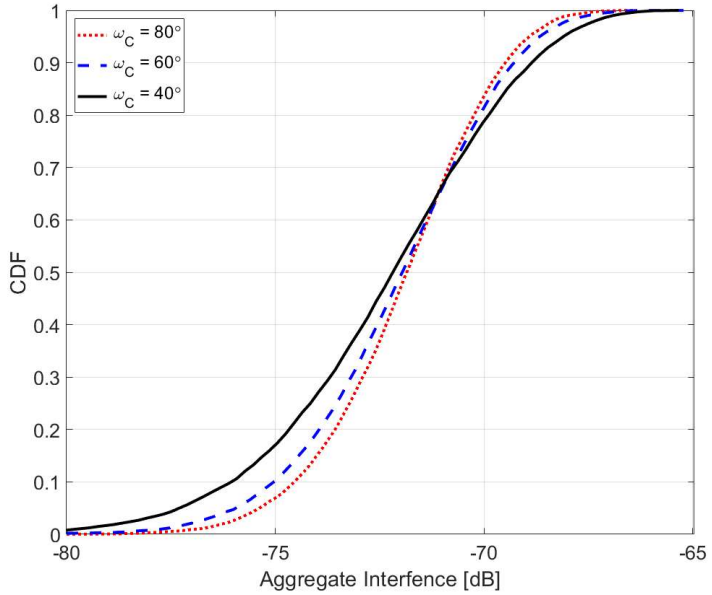

Figure 4-14: CDF of aggregated interference according to ω_C

4.3 QuaDRiGa based analysis

The aim of 5G-ALLSTAR, besides implementing a radio propagation model for LEO and GEO satellites, is to support coexistence simulations between terrestrial and satellite systems. This is especially important for the 5G era, where the Ka-band (26.5 – 40 GHz) might be partially used by terrestrial mobile radio communication systems. Hence, it is important to study the impact that the terrestrial usage of this band has on the satellite systems and vice-versa.

4.3.1 Simulation assumptions

For the space segment, two configurations are considered: one in GEO and one in LEO. The orbital parameters are chosen in a way that, seen from Earth, the satellite elevation angle for GEO is at about 45 degree and for LEO at about 90 degree. This approach has been suggested in 3GPP TR 38.821 [4]. For this, the origin on the local coordinate system is placed in the center of Spain at -5 deg latitude and 38.85 deg longitude. An overview of all satellite parameters is given in Table 4-2.

Table 4-2: Satellite parameters for stochastic simulations

Satellite orbit	GEO	LEO
Satellite altitude	35'786 km	600 km
Orbit inclination	0 deg	63.4 deg
Longitude of the ascending node	0 deg	-28.8 deg
Argument of periapsis	0 deg	44.55 deg
True anomaly	-5 deg	0 deg
Orbital period	24 hours	1 hour 37 minutes
Earth tangential plane origin	-5 deg latitude, 38.85 deg longitude	

The satellite creates a hexagonal grid of 19 beams using a reflector antenna with 19 feeds. The terrestrial network is placed in the center beam, whereas the surrounding 18 satellite beams cause interference to both. Here, we consider frequency reuse 1. The satellite beam configuration for S-band and Ka-band are shown in tables Table 4-3 and Table 4-4, respectively. Note that a carrier frequency of 25 GHz was chosen to simplify the simulations for uplink at 30 GHz and downlink at 20 GHz according to the assumptions by 3GPP [4].

Table 4-3: Satellite beam parameters for S-band simulations

Satellite orbit	GEO	LEO
Carrier frequency	2 GHz, 30 MHz bandwidth	
Satellite antenna aperture radius	11 m	1 m
Satellite antenna gain	51 dBi	30 dBi
3dB beamwidth	0.4011 deg	4.4127 deg
Satellite beam diameter on Earth	250 km	50 km
Satellite elevation angle	45 deg	90 deg
Satellite EIRP density	59 dBW/MHz	34 dBW/MHz
Satellite Tx power	190 W (52.8 dBm)	75 W (48.8 dBm)

Polarization	RHCP	RHCP
UE location	Outdoor LOS and NLOS	
UE antenna configuration	Handheld	

Table 4-4: Satellite beam parameters for Ka-band simulations

Satellite orbit	**GEO**	**LEO**
Carrier frequency	25 GHz, 400 MHz bandwidth	
Satellite antenna aperture radius	2.5 m	0.25 m
Satellite antenna gain	58.5 dBi	38.5 dBi
3 dB beamwidth	0.1765 deg	1.7647 deg
Satellite beam diameter on Earth	110 km	20 km
Satellite elevation angle	45 deg	90 deg
Satellite EIRP density	40 dBW/MHz	4 dBW/MHz
Satellite Tx power	5.65 W (37.5 dBm)	0.15 W (21.5 dBm)
Polarization	RHCP	RHCP
UE location	Outdoor LOS only	
UE antenna configuration	VSAT	

The terrestrial network consists of 57 cells within the central satellite beam. Terrestrial cells are assumed adjacent to each other. Two cases are distinguished in the way the satellite beam covers the cluster of terrestrial cells depending on the relative positions of the satellite and the ground area containing the cluster of terrestrial cells. Note that in any case, within the beam footprint (the spot) UEs are under different elevation angles, from 10° to 90°.

GEO - Central beam boresight direction computed based on 45 degree elevation angle target	**LEO** - Central beam center is considered at nadir point, i.e. directly below the satellite.
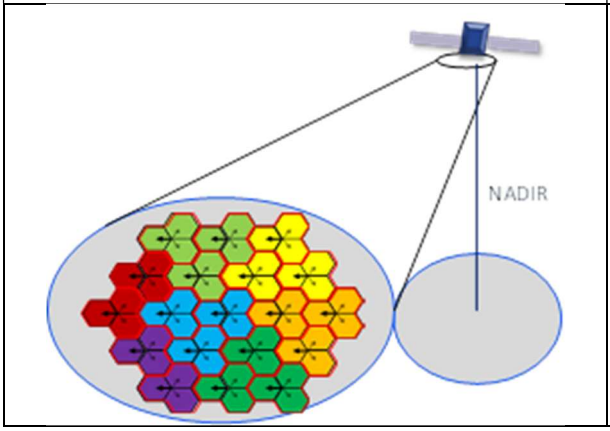	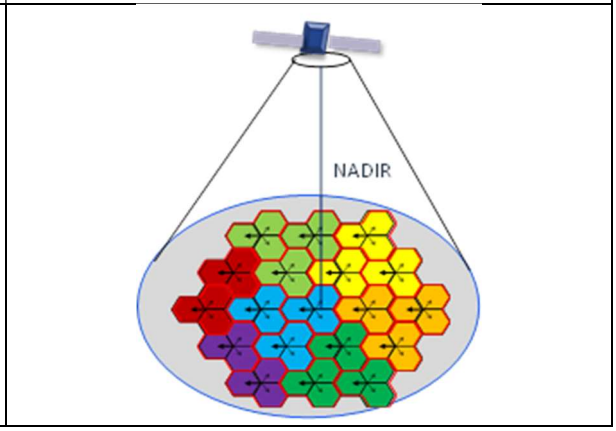

Figure 4-15: Satellite beam bore sight direction definition

The rationale behind the cell layout is the impact of the inter-cell interference. Terrestrial communication systems are inherently interference limited due to the isotropic antenna patterns at the UE. For this reason, beamforming techniques (either by tilted BS antennas or by precoding

techniques at the BS) are used to minimize the interference caused by other BSs in the radio link. To capture and evaluate the impact of the interference, a cell layout consisting of a hexagonal grid with 19 sites is chosen. The UEs are placed only within the central area, which is covered by the first ring of BSs. The outer ring provides a realistic interference scenario. Two sets of parameters are chosen for the terrestrial network as listed in Table 4-5. For the S-band, we assume a typical urban-macrocell deployment with 500 m inter-site distance and 25 m BS height. For the Ka-band, we assume an urban-microcell deployment with 200 m inter-site distance and 10 m BS height. In both cases, UEs are assumed to be handheld devices with linear polarized omnidirectional antennas. However, for the Ka-band, we assume that the UEs must have a LOS connection to their serving BS, whereas in S-band, LOS and NLOS links are considered.

Table 4-5: Terrestrials network parameters

Satellite orbit	S-band (UMa)	Ka-band (UMi)
Carrier frequency	2 GHz	25 GHz
Bandwidth	30 MHz	400 MHz
Cell layout	Hexagonal grid, 19 sites, 3 sectors per site	
Inter-site distance	500 m	200 m
BS antenna height	25 m	10 m
BS antenna configurations	10 stacked elements, 0.5 lambda spacing, fixed beam	
BS antenna gain	17.3 dBi	17.3 dBi
BS antenna electrical downtilt	12 deg	12 deg
BS Tx power	25.1 W (44 dBm)	3.2 W (35 dBm)
Polarization	Linear : +/-45°X-pol	Linear : +/-45°X-pol
UE location	Outdoor LOS and NLOS	Outdoor LOS only
UE antenna configuration	Handheld	Handheld

We consider two configurations for the UE antenna: one for direct access to the UE which is used by all terrestrial links and satellite links in S-band (Handheld) and one for satellite access using a very small aperture terminal (VSAT) in Ka-band. The UE characteristics are listed in Table 4-6.

Table 4-6: UE characteristics

UE Type	Handheld S-band / Ka-band	VSAT Ka-band (UMi)
Carrier frequency	2 GHz / 25 GHz	25 GHz
Antenna type and configuration	Dual-polarized omnidirectional antenna elements	Directional reflector antenna-with 60 cm equivalent aperture diameter
Polarisation	Linear : +/-45°X-pol	RHCP
Antenna gain	0 dBi per element	39.7 dBi
Antenna temperature	290 K	150 K
Noise figure	7 dB	1.2 dB

Tx transmit power	0.2 W (23 dBm)	2 W (33 dBm)

4.3.2 Evaluation Metrics

When several transmitters use the same time and frequency resources, they create interference. A receiver will not only receive the signal from its serving transmitter but also signals from other interfering devices as well. The correct prediction of the signal strength is therefore an important criterion for channel models. The geometry factor (GF) is the lower bound for the instantaneous SINR. It does not consider the effects of fast-fading and possible gains of scheduling in the frequency domain. It is defined as the average power ratio of the serving BS to the average power of all interfering BSs plus noise.

$$GF = \frac{P^{[signal]}}{P^{[noise]} + P^{[interference]}}.$$

Due to handover, the UE is always assigned to the serving transmitter with the highest received power in its class (e.g. a cellular UE can only connect to BSs). The average received signal power is calculated as

$$P^{[signal]} = P^{[tx]} + \frac{1}{n_t} \cdot \sum_{r=1}^{n_r} \sum_{t=1}^{n_t} \sum_{l=1}^{L} \left| g_{r,t,l} \right|^2,$$

where r, t and l are the indices of the receive antenna element, the transmit antenna element, and the multipath-component, respectively. $P^{[tx]}$ is the total average transmit power of the serving gNB or satellite beam. The antenna gains are not calibrated out of the data since they have a tremendous influence on the GF. The thermal noise power $P^{[noise]}$ is calculated in dBm as

$$P^{[noise]}{}_{\mathrm{dBm}} = -174 + 10 \cdot \log_{10} B + \mathrm{NF},$$

where B is the bandwidth in Hz and NF is the noise figure.

4.3.3 Simulation steps

In order to evaluate all 8 interference scenarios listed in Section 2.1, simulations are set-up in the following way:

1. Generation of the cellular network

   The terrestrial network consists of 19 base-stations, each having 3 sectors. The resulting 57 cells are assumed adjacent to each other. The BS antenna has a gain of 17.3 dBi and is electrically tilted by 12 degree. The intersite distance is set to 500 m in S-band and 200 m in Ka-band. No additional beamforming is assumed. The geometry of the terrestrial system in S-band is shown in Figure 4-16, where the GF in dB is shown as a background image. We assume that no frequency reuse (frequency reuse factor equals one) is applied. Hence, there is significant interference from other cells.

2. Generation of the satellite network

   Two satellites are placed in orbit using the parameters from Table 4-2. The elevation target is set to 45 degree for GEO and 90 degree for LEO. The antenna characteristics are set as described in Table 4-3 and Table 4-4. Figure 4-17 shows the network geometry for the GEO setup in Ka-band. Note that satellite cells are much larger (110 km diameter in the figure) compared to terrestrial cells. Hence, the entire terrestrial network fits into the center blue dot in Figure 4-17. Similar geometries are achieved for the other satellite network types but with different beam diameters.

3. Interfering UEs

The UEs on the ground can either communicate with the terrestrial network (cellular UE), the GEO satellite (GEO UE) or the LEO satellite (LEO UE) or they cause interference. In order to estimate the interference caused by these UEs, we need to make assumptions about their placement, orientation and resource allocation. For the sake of simplicity, we randomly place 300 interfering UEs into the center ring of BSs as shown by the blue dots in Figure 4-16. These UEs are subdivided into the 3 classes: 100 cellular UEs, 100 GEO UEs and 100 LEO UEs. In S-band, they are all equipped with handheld antennas having omnidirectional antennas. Hence, their orientation is unimportant. However, in Ka-band, the GEO and LEO UEs use VSAT antennas pointed towards the satellite. Each UE uses the full bandwidth (30 MHz in S-band or 400 MHz in Ka-band) and transmits with full power. The effects of different traffic patterns and resource allocation schemes such as scheduling are not considered here and might be subject to further study.

4. Receiving UEs

   600 UEs are randomly placed into the center ring of the terrestrial BSs as receivers. As for the interfering UEs, these are divided into cellular UEs, GEO UEs and LEO UEs. Additional 19 receivers are collocated with the BSs. These are for calculating the interference levels seen at the BSs. They have 6 antennas in a dual-polarized set-up resembling a 3-sector configuration.

5. Scenario assignment

Each link gets assigned a scenario as listed in Table 4-7.

Table 4-7: Scenario Assignment for QuaDRiGa simulations

Node A	Node B	Band	Scenario
Satellite	UE	S	5G-ALLSTAR D3.1 Suburban LOS and NLOS, [27]
Satellite	UE	Ka	5G-ALLSTAR D3.1 Suburban LOS, [27]
Satellite	gNB	S / Ka	Free space
gNB	UE	S	3GPP UMa LOS and NLOS, [1]
gNB	UE	Ka	3GPP UMi LOS, [1]
UE	UE	S / Ka	QuaDRiGa UD2D LOS and NLOS

The results are presented and discussed in Section 4.3.4.

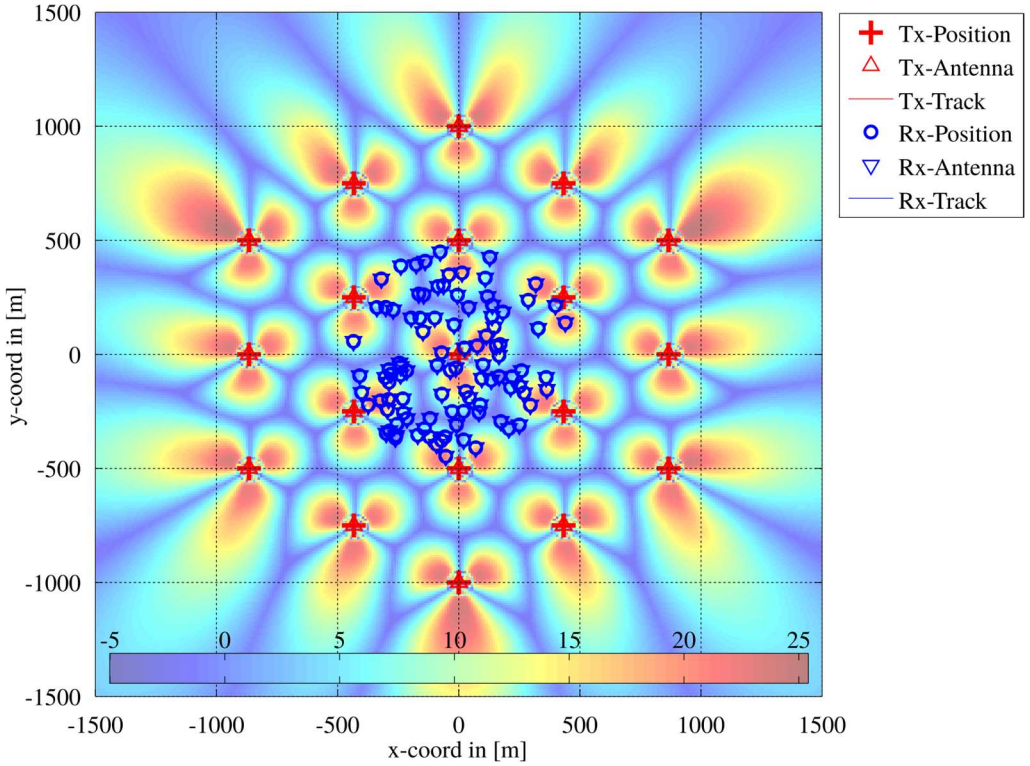

Figure 4-16: Terrestrial Network Geometry in S-band

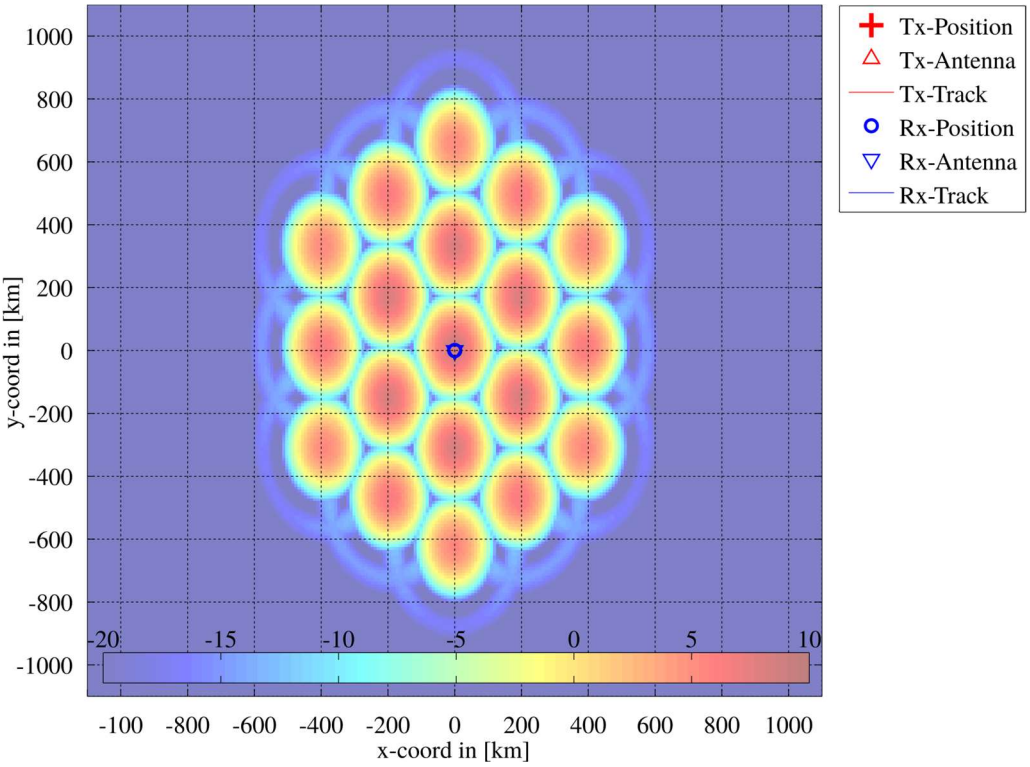

Figure 4-17: GEO Satellite Network Geometry in Ka-band

4.3.4 Results

This section presents the results for the eight interference scenarios introduced in Section 2.1. Simulations are done for the two frequency bands: S-band and Ka-band and for two satellite types, one in GEO and one in LEO. The simulation assumptions are described in Section 4.3.1.

The first step was to estimate the achievable SNR taking into account the transmit power, transmit antenna gain, orientation, path loss, receive antenna gain and noise figure for each combination of transmitter and receiver. The median values are listed in Table 4-8 for the S-band and in Table 4-9 for the Ka-band. Median values were chosen since the values can be easily converted from dB to linear scale while keeping their meaning as opposed to mean values. Values highlighted in bold font are for the intended link. Values in green indicate a "good" combination of parameters (i.e. high serving link budget, low interference), values in red indicate the opposite.

Table 4-8: Median SNR (dB) in S band

Transmitter	Receiver					
	Cell. gNB	GEO Sat.	LEO Sat.	Cell. UE	GEO UE	LEO UE
Cell. gNB	-	-5	-25	**42**	42	42
GEO Sat.	-22	-	-	6	**6**	6
LEO Sat.	-26	-	-	17	17	**17**
Cell. UE	**21**	-18	-3	-	50	50
GEO UE	21	**-18**	-3	50	-	50
LEO UE	21	-18	**-3**	50	50	-

In the S-band, all UEs are equipped with omnidirectional antennas, i.e. there is no gain in certain directions. This can be seen in Table 4-8, where all 3 UE types experience the same SNR for a selected transmitter type. The gNB has a 17.3 dBi antenna gain, 44 dBm transmit power and 500 m inter-site distance (ISD). This combination achieves a median SNR of 42 dB at the UEs. This seems to be too high for practical purposes. The interference experienced by the satellite UEs is enormous. They could establish a link with the satellite (at 6 dB SNR for GEO and 17 dB for LEO), but only if there were no BSs or UEs using the same frequency band. In the uplink, the missing antenna gain of the satellite UEs combined with the 23 dBm transmit power for handheld UEs leads to a negative SNR when the UEs use the full bandwidth, especially for GEO UEs.

Table 4-9: Median SNR (dB) in Ka-band

Transmitter	Receiver					
	Cell. gNB	GEO Sat.	LEO Sat.	Cell. UE	GEO UE	LEO UE
Cell. gNB	-	-40	-59	**28**	-6	0
GEO Sat.	-62	-	-	-36	**9**	-114
LEO Sat.	-78	-	-	-36	-128	**10**
Cell. UE	**16**	-44	-29	-	-10	-13
GEO UE	-14	**4**	-117	0	-	-84
LEO UE	-8	-119	**21**	-9	-86	-

In Ka-band, the satellite UEs use directional antennas with 39.7 dBi gain pointed towards the satellite. This significantly reduces the interference levels. Satellite UEs can significantly reduce the interference from gNBs but this might still not be sufficient considering the lower transmit power at the satellite compared to the terrestrial network.

In the following, results for the 8 interference scenarios are presented and discussed. An overview is given in Table 4-10 for the S-band and Table 4-11 for the Ka-band. The tables list the median values and the 10% quantile (Q10) of the empirical CDF, i.e. the minimum value that the worst 10% of the UEs have to cope with. Interference is caused by the communication system itself and by an additional external interferer. If the external interferer is "off", the GF is calculated for interference within the same system only, i.e. cellular UEs experience interference from other cellular gNBs. If the external interferer is "on", the additional interference is added, i.e. cellular UEs experience interference from other cellular gNBs and from satellite UEs using the same frequency band. Hence, external interference will always lead to a lower GF.

Table 4-10: Geometry Factors (dB) in S band

				GEO (Med)		LEO (Med)		GEO (Q10)		LEO (Q10)	
Scen.	**Rx**	**Tx**	**Interferer**	off	on	off	on	off	on	off	on
1a	Cell UE	Cell gNB	Sat UE	3.8	-6.1	3.8	-8.8	-2.0	-25.4	-2.0	-25.1
1b	Cell gNB	Cell UE	Sat UE	-4.8	-25.1	-4.8	-25.1	-24.2	-43.3	-24.2	-41.8
1c	Cell UE	Cell gNB	Satellite	3.8	3.8	3.8	3.8	-2.0	-2.0	-2.0	-2.0
1d	Cell gNB	Cell UE	Satellite	-4.8	-4.8	-4.8	-5.8	-24.2	-24.2	-24.2	-24.2
2a	Sat UE	Satellite	Cell UE	10.2	-46.9	14.8	-33.8	7.4	-60.3	13.8	-43.8
2b	Sat UE	Satellite	Cell gNB	10.2	-38.1	14.8	-26.8	7.4	-60.4	13.8	-45.9
2c	Satellite	Sat UE	Cell UE	-18.3	-24.3	-3.5	-23.4	-20.4	-26.3	-5.1	-25.1
2d	Satellite	Sat UE	Cell gNB	-18.3	-19.5	-3.5	-3.5	-20.4	-21.6	-5.1	-5.2

Table 4-11: Geometry Factors (dB) in Ka-band

				GEO (Med)		LEO (Med)		GEO (Q10)		LEO (Q10)	
Scen.	**Rx**	**Tx**	**Interferer**	off	on	off	on	off	on	off	on
1a	Cell UE	Cell gNB	Sat UE	3.4	3.1	3.4	3.1	-1.6	-2.1	-1.6	-2.2
1b	Cell gNB	Cell UE	Sat UE	3.2	-0.9	3.2	-5.8	-4.3	-11.9	-4.3	-19.6
1c	Cell UE	Cell gNB	Satellite	3.4	3.4	3.4	3.4	-1.6	-1.6	-1.6	-1.6
1d	Cell gNB	Cell UE	Satellite	3.2	3.2	3.2	3.2	-4.5	-4.5	-4.5	-4.5
2a	Sat UE	Satellite	Cell UE	7.8	6.0	8.7	7.2	4.2	-3.0	5.8	-3.7
2b	Sat UE	Satellite	Cell gNB	7.8	5.2	8.7	5.1	4.2	-4.5	5.8	-15.6
2c	Satellite	Sat UE	Cell UE	4.0	4.0	21.2	19.9	0.0	0.0	17.8	16.4
2d	Satellite	Sat UE	Cell gNB	4.0	4.0	21.2	21.2	0.0	0.0	17.8	17.8

Case 1a - From satellite UE to cellular UE

The cellular gNB serves the cellular UE in the downlink. Satellite UE use the same frequency band for their uplink communication towards the satellite. This causes interference at the cellular UE. The empirical CDF of the geometry factor in this case are shown in Figure 4-18.

The S-band UEs use omnidirectional antennas. Hence, they radiate their signals in all directions causing massive distortions for nearby cellular UEs. The GF drops from a median value of 3.8 dB to -6.1 dB when satellite UEs are active. Cellular UE most likely will not be able to tolerate this interference. In the Ka-band, satellite UEs use directional VSAR antennas with 39.7 dBi gain. They are pointed directly towards the satellite. The interference caused for the cellular UEs is minimal.

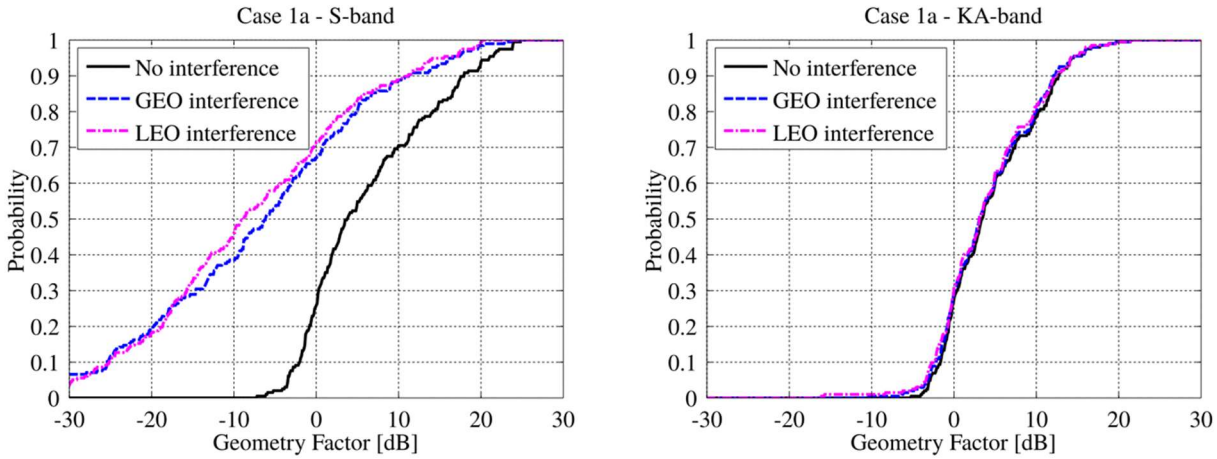

Figure 4-18: Geometry factor CDF for case 1a - satellite UE to cellular UE

Case 1b - From satellite UE to cellular gNB

The cellular UE transmits towards the cellular gNB in the uplink. For the calculation of the GF, we assume that the UE uses the whole bandwidth in the uplink. This is not realistic for LTE or 5G deployments where a more sophisticated resource allocation scheme is used. The interference of neighbouring terrestrial cells is estimated by using the average power of all UEs assigned to this cell. Satellite UE use the same frequency band for their uplink communication towards the satellite. This causes additional interference at the cellular gNB. We assume that 100 satellite UEs transmit with full power at the same time.

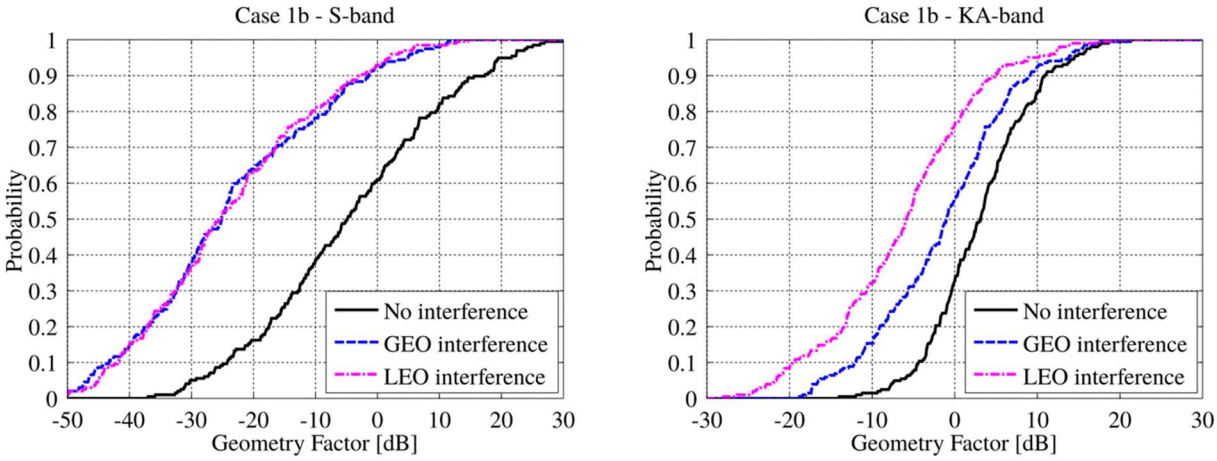

Figure 4-19: Geometry factor CDF for case 1b - satellite UE to cellular gNB

In the S-band, the cellular system achieves a median GF of only -4.8 dB without interference from satellite UEs. This is not a realistic value since in practice, we need to account for the fact that UEs use a much smaller uplink bandwidth and hence achieve a better power-spectral density. Further studies need to take this into account. For more realistic results, we also need to consider that inter-cell optimization is done to reduce the interference levels from neighbouring cells. However, when adding uncoordinated interference from 100 satellite handheld UEs, we can observe a 20 dB lower GF compared to the standalone cellular system.

In Ka-band, the shorter range of the terrestrial communication system improves the situation for standalone terrestrial communication, leading to a similar GF as in the downlink. However, satellite UEs create significant interference despite their directional antennas. This might come from the fact, that the BSs are at an elevated position and that significant energy from the satellite UEs feeds into the high-gain BS antennas.

Case 1c - From satellite to cellular UE

This case considers interference from the satellite at the cellular UE. However, there is none. The satellite signals are too weak compared to the signal received from the cellular gNB to have any impact on the cellular network performance.

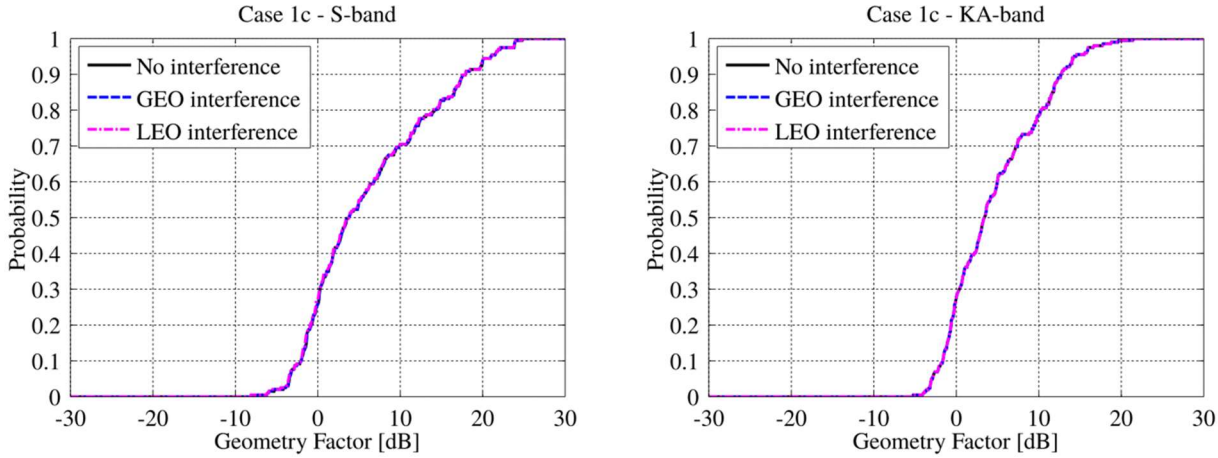

Figure 4-20: Geometry factor CDF for case 1c - satellite to cellular UE

Case 1d - From satellite to cellular gNB

Similar to case 1c, this case considers the interference of the satellite signal on the uplink transmission in the cellular system. As for the downlink, there is no significant impact on the cellular network.

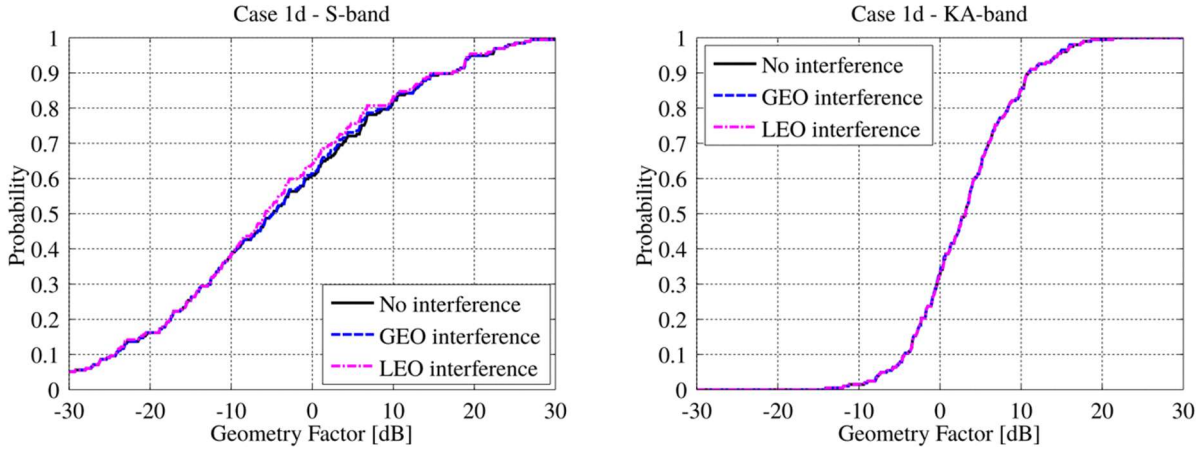

Figure 4-21: Geometry factor CDF for case 1d - satellite to cellular gNB

Case 2a - From cellular UE to satellite UE

The satellite serves the satellite UE in the downlink. The satellite signals are very weak. Without terrestrial interference, all satellite links have a GF above 4 dB with median values around 10

dB in S-band and 8 dB in Ka-band. Cellular UEs use the same frequency band for their uplink communication towards the gNB. This causes interference at the satellite UE.

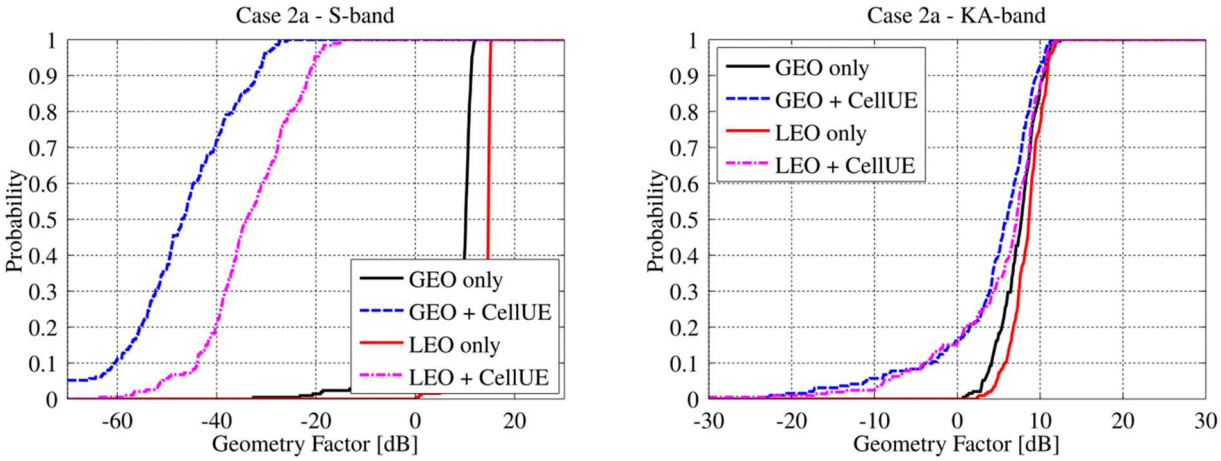

Figure 4-22: Geometry factor CDF for case 2a - cellular UE to satellite UE

The S-band UEs use omnidirectional antennas. Hence, they radiate their signals in all directions causing massive distortions for nearby satellite UEs. The GF drops from a median value of 10 dB to -46 dB (GEO) when satellite UEs are active. Satellite UEs will not be able to tolerate this interference. In the Ka-band, satellite UEs use directional VSAT antennas with 39.7 dBi gain. They are pointed directly towards the satellite. For most UEs, the interference caused by terrestrial handheld UEs is tolerable. However, there are some UEs that suffer significantly. 10% of the UEs experience a GF drop of 7 dB or more.

Case 2b - From cellular gNB to satellite UE

The satellite serves the satellite UE in the downlink. Cellular gNBs use the same frequency band for their downlink communication towards the handheld UEs. The situation is similar to the one in case 2a: S-band UEs are not able to tolerate the interference at all. Their GF drops by more than 40 dB. In the Ka-band, the situation is improved by the directional VSAT antennas that are pointed towards the satellite. However, the cellular gNB are at an elevated position, directing their signals towards the handheld UEs on the ground. This leads to a significant drop in performance for roughly 40% of the Ka-band satellite UEs. The situation is slightly better for LEO UEs which point their antennas straight up.

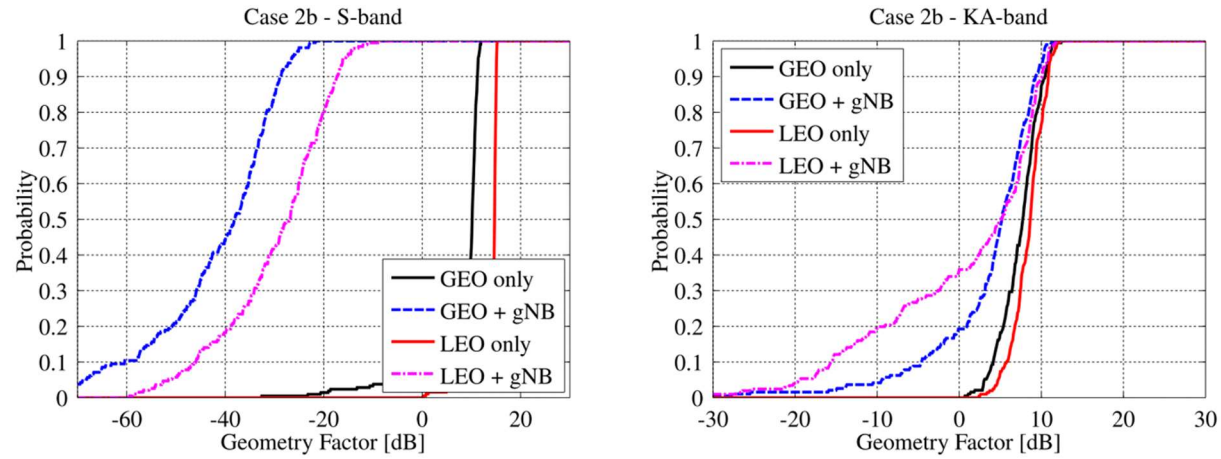

Figure 4-23: Geometry factor CDF for case 2b - From cellular gNB to satellite UE

Case 2c - From cellular UE to satellite

The satellite UE transmits towards the satellite in the uplink. For the calculation of the GF, we assume that the UE uses the whole bandwidth in the uplink and only one UE is active at any time. There is no interference from UEs in neighbouring satellite beams since the simulation layout does not consider this. However, the satellite GF in Figure 4-17 indicates the uplink GF should have values of up to 10 dB when UEs are in the center of the beam. This is similar to downlink SNR.

In the S-band, handheld UEs have no antenna gain and their transmit power is limited to 23 dBm. That leads to extremely poor performance with an average interference-free GF of only -18 dB for GEO UEs and -3 dB for LEO. Additional interference from cellular UEs lowers these values to around -25 dB. Establishing a communication link under these conditions will be challenging. In the Ka-band, the situation is much better. The 39.7 dBi gain of the VSAT antenna combined with the 33 dBm transmit power leads to a stable uplink connection. The antenna gain also combats the interference from the cellular UEs efficiently.

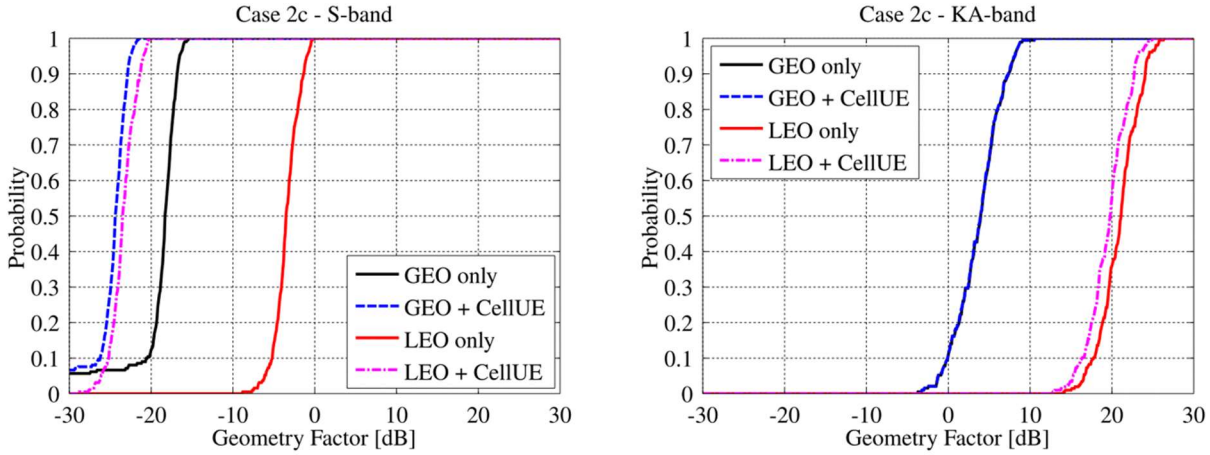

Figure 4-24: Geometry factor CDF for case 2c - cellular UE to satellite

Case 2d - From cellular gNB to satellite

In the last case, the satellite UE transmits towards the satellite in the uplink and interference is caused by terrestrial gNBs communicating with the handheld UEs in the downlink. The same performance limitations apply in the S-band as describes in case 2c. However, since the gNB uses directional antennas pointed towards the ground, little interference is experienced by the satellite. However, this might not be the case when very low elevation angles are considered as well.

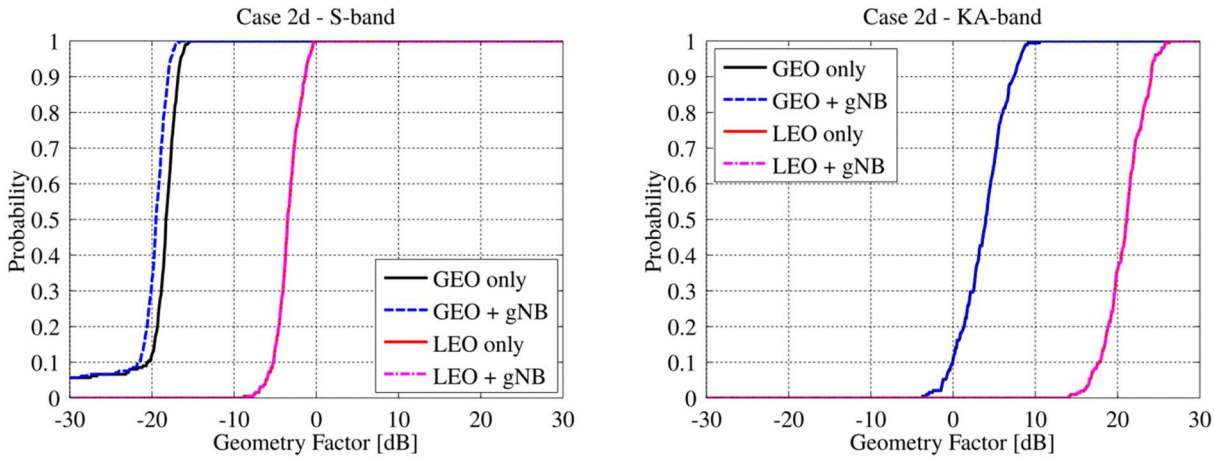

Figure 4-25: Geometry factor CDF for case 2d - cellular gNB to satellite

4.4 Ray-tracing-based analysis

4.4.1 Simulation assumptions

For the ray-tracing based approach, we consider the interference at the UE side in two environments, i.e. urban and highway, both located in Seoul, Korea. The carrier frequency for both systems, terrestrial and satellite, is set to 22.6 GHz with a bandwidth of 1 GHz.

For urban scenario, the Tx is placed on top of a building at a height of 25 m. For the highway scenario, the Tx is placed on a traffic light at a height of 10 m. As shown in Figure 4-26, the Rx is placed on top of a bus at a height of 3.2 m (bus height: 3 m) located 0.1 m from the rear. The travel distance of the bus is 500 m for both, urban and highway scenarios. The bus is assumed to be served by the terrestrial system and hence considered as cellular UE.

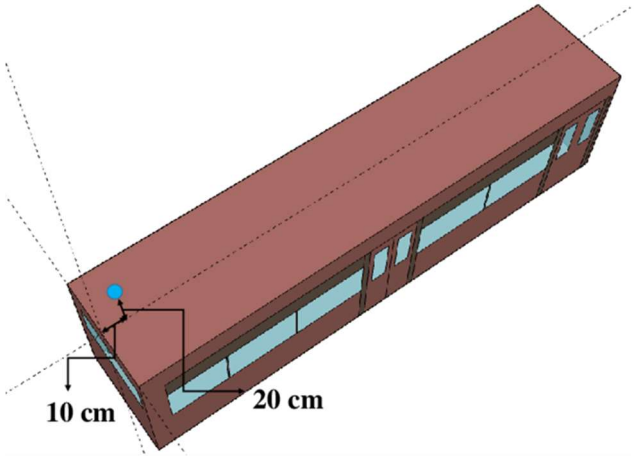

Figure 4-26: Rx location at a bus for terrestrial system

In addition to the cellular UE, a second UE in form of an SUV is placed in the scene. The communication scenario and the travel track are the same as for the bus. The SUV is assumed to be served by a satellite, making it a satellite UE. As a realistic example we assume Koreasat 6 as the serving satellite. Koreasat 6 is a GEO satellite, positioned at 116 ° E 35786 km above the equator. The distance from the satellite to the target area in Seoul is approximately 37470

km. As shown in Figure 4-27, the Rx is mounted on top of it at a height of 2.4 m (SUV height: 1.75 m) located 1.48 m from the rear.

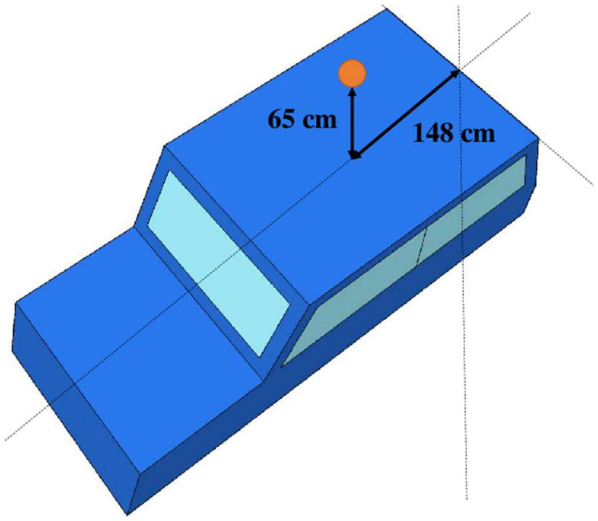

Figure 4-27: Rx location at an SUV for satellite service

Table 4-12 and Table 4-13 describe the scenario configurations for the assumed terrestrial and satellite systems. The communication scenarios for both systems are almost the same. The main differences are the locations of the Tx and the selected antennas for Tx and Rx. The ray-tracer considers the direct path, as well as reflected, scattered, diffracted, and refracted paths.

Table 4-12: Scenario configuration for terrestrial system

Frequency	22.1 – 23.1 GHz		
Bandwidth	1 GHz		
Antenna	Directional antenna		
Tx	Power		20 dBm
	Maximum antenna gain		16 dBi
	Antenna beamwidth		20 degrees
	Height	Urban scenario	25 m
		Highway scenario	10 m
Rx	Maximum antenna gain		22 dBi
	Antenna beamwidth		20 degrees
	Height		3.2 m
	Travel distance for urban scenario		500 m
	Travel distance for highway scenario		500 m
V2I path	D1: Rx on the Lane 3 (4-lane urban street)		
	D2: Rx on the Lane 5 (8-lane highway)		
Vehicle type	Bus	Shown in Figure 4-26	

Table 4-13: Scenario configuration for satellite link

Frequency	22.1 – 23.1 GHz		
Bandwidth	1 GHz		
Antenna	Directional antenna		
Tx	Power		40.6 dBm
	Maximum antenna gain		53 dBi
	Antenna beamwidth		1 degree
	Approximate distance to Rx		37469.3 km
Rx	Maximum antenna gain		32 dBi
	Antenna beamwidth		3 degrees
	Height		2.4 m
	Travel distance for urban scenario		500 m
	Travel distance for highway scenario		500 m
V2I path	D1: Rx on the Lane 3 (4-lane urban street)		
	D2: Rx on the Lane 5 (8-lane highway)		
Vehicle type	SUV	Shown in Figure 4-27	

Frequency reuse and interference are a set of indivisible themes. Due to the fact that the terrestrial and the satellite system use the same spectrum in this task, co-channel interference exists between the satellite network and the terrestrial network. Co-channel interference means the carrier frequencies of the desired signal and the interference signal are the same and are received by the receiver without discrimination, which increases the difficulty in detecting the desired signal.

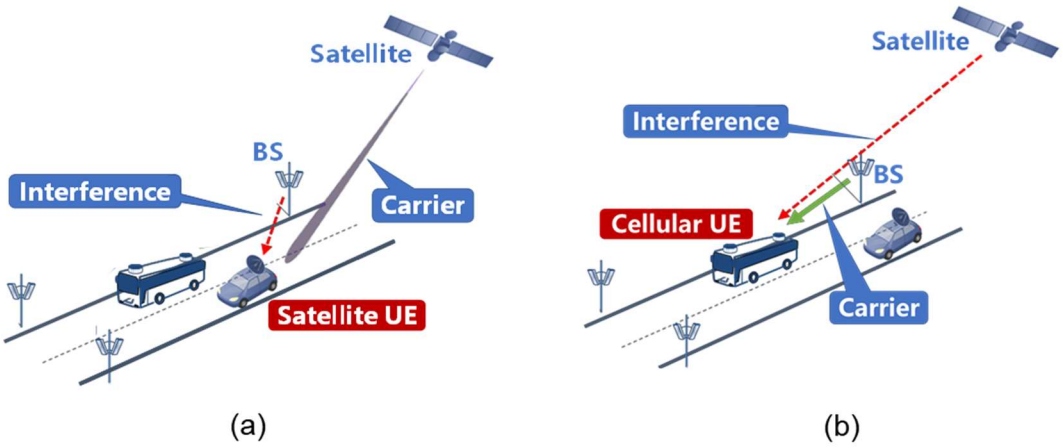

Figure 4-28: Co-channel interference situations in urban and highway scenarios: a) BS-to-satellite UE interference; b) Satellite-to-cellular UE interference

Based on the simulation, two kinds of co-channel interference situations in urban and highway scenarios need to be considered, as presented in Figure 4-28, where (a) represents the interference from the terrestrial system to the satellite system and (b) represents the interference from the satellite system to the terrestrial system. The 4 cases are summarized in Table 4-14 for clarity.

Table 4-14: Co-channel interference analysis cases

Scenario	Carrier	Interference
Seoul urban1	SA2SaUE	BS2SaUE
	BS2VeUE	SA2VeUE
Highway	SA2SaUE	BS2SaUE
	BS2VeUE	SA2VeUE

4.4.2 Results

The carrier-to-interference ratio (C/I) is the quotient between the carrier received power and interference received power, as defined in Section 3. The results of C/I for all the interference cases defined in Table 4-14 are shown in Figure 4-29 and Figure 4-30.

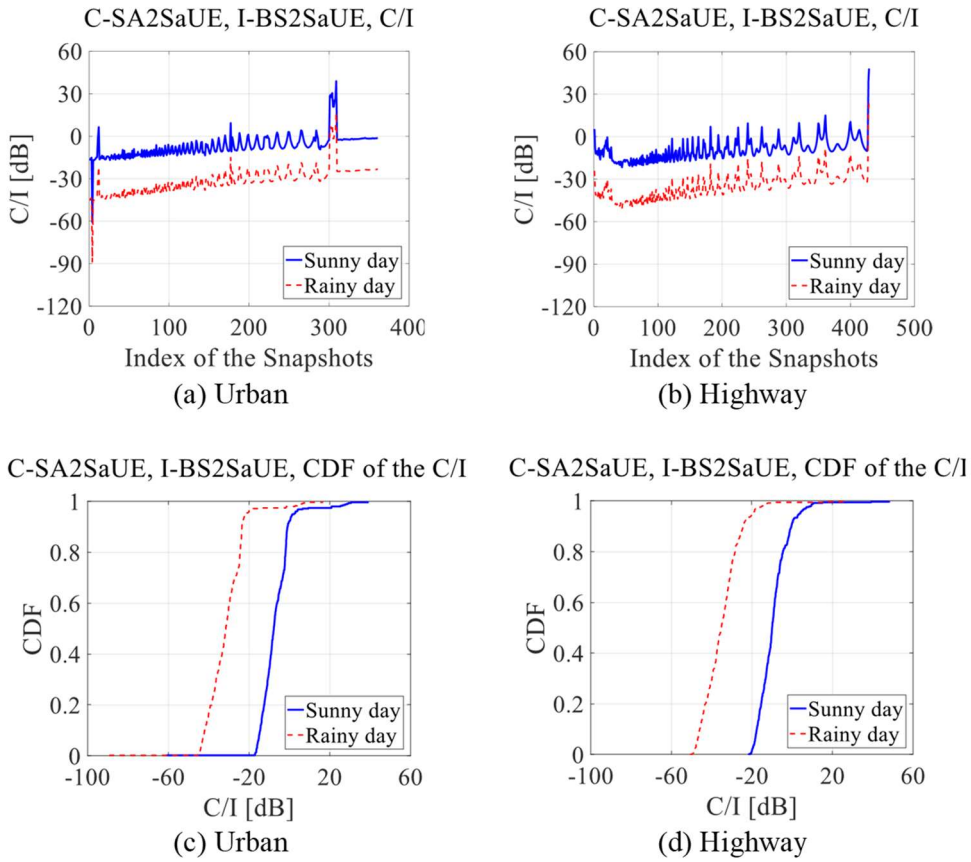

Figure 4-29: Cellular interference to the satellite system

Figure 4-29 shows the C/I CDF of the considered interference cases. The red dotted lines represent the minimum C/I in rainy day. The blue solid lines represent the C/I in the sunny day. Since the rain attenuation of the satellite link is more significant, the C/I will increase as the rain attenuation decreases.

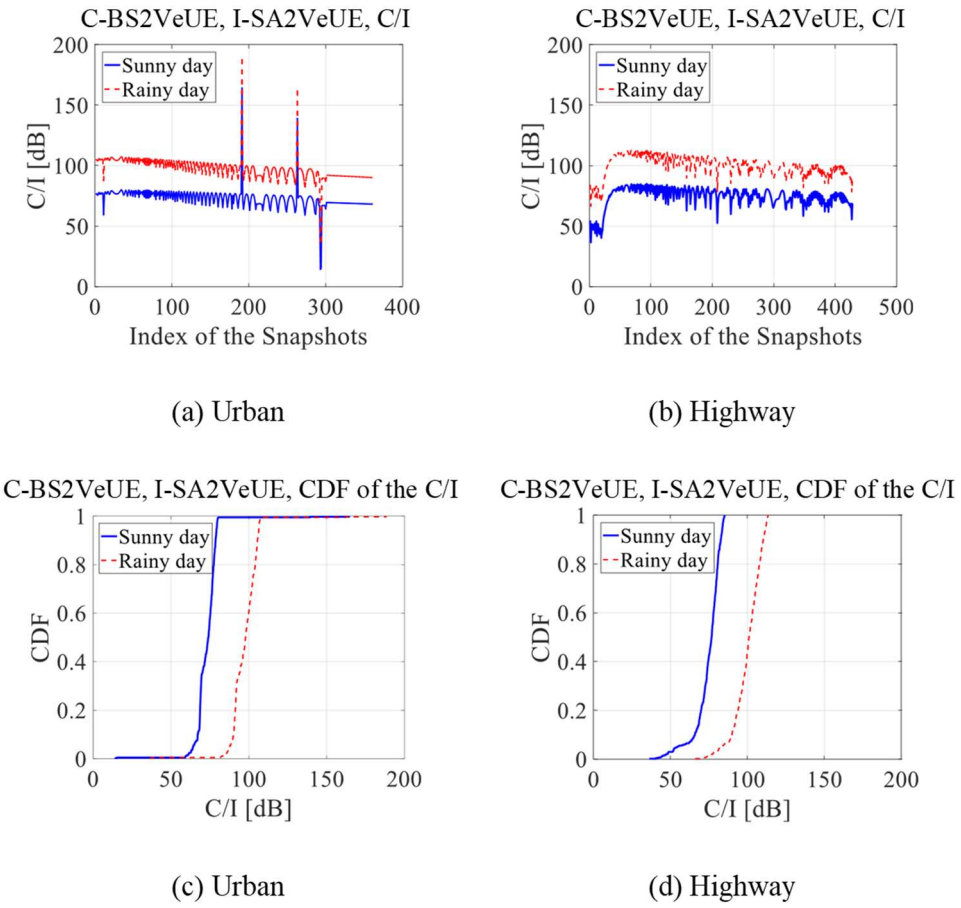

Figure 4-30: Satellite interference to the terrestrial system

However, when treating the terrestrial system downlink as the carrier and the satellite downlink as interference, then the influence of rain attenuation on the interfering link is much greater than that on the carrier. As shown in Figure 4-30, the C/I will decrease as the rain attenuation diminishing.

Comparing Figure 4-29 and Figure 4-30, following conclusions can be drawn: when treating the satellite downlink as the carrier and the terrestrial system downlink as the interference, the C/I is often less than 0 dB (as shown in Figure 4-29). When the terrestrial system downlink is the carrier and the satellite downlink is the interference, the C/I is basically larger than 20 dB (as shown in Figure 4-30). This indicates that the satellite downlink has almost no impact on the terrestrial system downlink, but the interference of the terrestrial system downlink on the satellite downlink is significant. Therefore, it seems most beneficial to develop interference mitigation techniques for reducing the impact of the link from BSs to satellite UEs.

5 Adjacent channel interference analysis

In this section, the adjacent channel interference scenario is considered, see Figure 2-4: interference of system B on system C. As most of the interference is concentrated in the edges of the spectrum, the most impacting factor is the out-of-band rejection capability of the waveform: the performance of Cyclic Prefix OFDM (CP-OFDM) in this context are assessed.

More specifically, case c) of Figure 2-1, gNB to satellite UE interference is studied. This case is of major interest, as demonstrated in Figure 5-1, extracted from [27]: the power received at the satellite UE from the gNB (the interference) is much higher than the power received from the satellite.

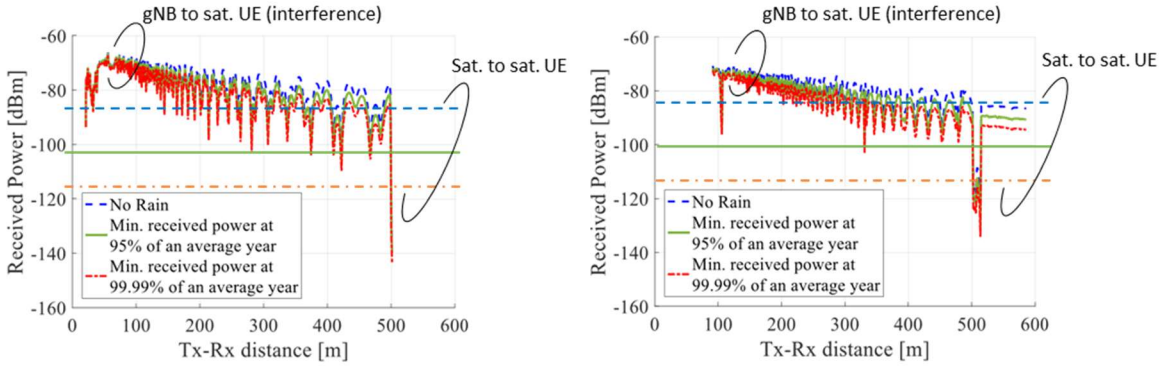

Figure 5-1: Received power at the satellite UE, highway (left) and urban (right) scenarios, [27]

Based on [27] the parameters of the simulation are derived, see Table 5-2:

- The waveform is CP-OFDM; the goal of this study is to assess the performance of this waveform in a context of spectrum sharing without any filtering stage. CP-OFDM will be compared to waveforms using filtering techniques in deliverable 3.3.
- The carrier frequency, 22.5 GHz, is consistent with the simulations from [27].
- The terrestrial system uses numerology 2; for the satellite system numerologies 2 and 3 are assessed. For each 5G NR numerology, the inter-carrier spacing Δ_f, the OFDM symbol duration T_u^{μ}, the cyclic prefix duration T_{CP}^{μ} and the number of slots per frame $N_{slot}^{frame,\mu}$ are recalled in Table 5-1.

Table 5-1: 5G NR numerologies

μ	Δ_f $[kHz]$	T_u^{μ} $[\mu s]$	T_{CP}^{μ} $normal$ $[\mu s]$		$N_{slot}^{frame,\mu}$
			$l = \{0, 7 \cdot 2^{\mu}\}$*	$l \neq \{0, 7 \cdot 2^{\mu}\}$*	
0	15	66.66	5.21	4.69	10
1	30	33.33	2.86	2.34	20
2	60	16.66	1.69	1.17	40
3	120	8.33	1.11	0.59	80
4	240	4.16	0.81	0.29	160

* l is the OFDM symbol number in a subframe (1 ms).

- In adjacent channel systems, the interference is maximal on the spectrum edges; we can therefore expect the performance to vary with the width of the bandwidth. The performance are then evaluated with two bandwidths, see Figure 5-2: 15.36 MHz and 30.72 MHz.
- The terrestrial Modulation and Coding Scheme (MCS) is #22 (64-QAM rate 666/1024). A range of MCS are assessed for the satellite system, the most robust MCSs for the

urban scenario are #2 (QPSK 193/1024) and #5 (QPSK 379/1024); and #5, #10 (16-QAM 340/1024) and up to #15 (16-QAM 616/1024) for the highway scenario.

- The guard band, see Figure 5-2, ranges from 0 kHz to 960 kHz.
- In order to reflect the differences between the terrestrial and the satellite received powers (see Figure 5-1), the parameter ΔP, see Figure 5-2, is set to {45, 10, 5, 0} dB.
- The channel models reflect the simulated environments:
    - For the highway scenario, the terrestrial channel model is TDL-D 100 as defined in [1], and the satellite channel model is Vehicular Open Rural with a K-Factor of 20 dB. The receiver speed is 110 km/h (the Doppler is simulated based on the sum of sinusoids method).
    - For the urban scenario, the terrestrial channel model is TDL-B 100 as defined in [1], and the satellite channel model is Vehicular Quasi-Open Rural with a K-Factor of 8 dB. The receiver speed is 50 km/h (the Doppler is simulated based on the sum of sinusoids method).

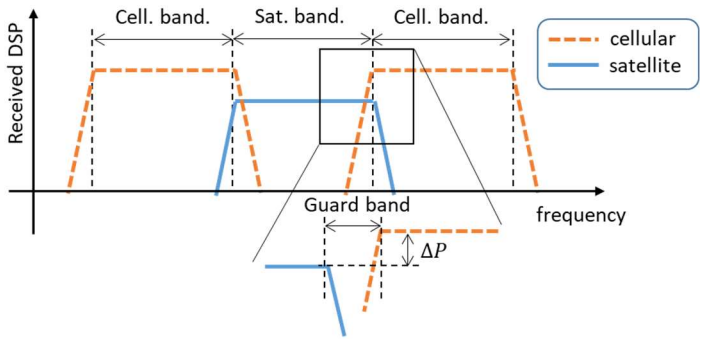

Figure 5-2: Simulated scenario and parameters

Table 5-2: Adjacent channel interference parameters

Parameter	Highway	Urban
Waveform	CP-OFDM	
Fc	22.5 GHz	
μ satellite	{2,3}	
μ cellular	2	
Satellite bandwidth	{15.36, 30.72} MHz	
Cellular bandwidth	{15.36, 30.72} MHz	
MCS satellite	{15, 10, 5}*	{5, 2}*
MCS cellular	22*	
Guard band	{0,60,120,240,480,960} kHz	
Cellular on Satellite received power ΔP	{45,10,5,0} dB	
Channel satellite	Veh. open rural K=20 dB	Veh. quasi-open rural K=8 dB
Channel cellular	TDL-D 100**	TDL-B 100**
Speed	110 km/h	50 km/h

* **MCS 2**: QPSK 193/1024; **MCS 5**: QPSK 379/1024; **MCS 10**: 16-QAM 340/1024; **MCS 15**: 16-QAM 616/1024; **MCS 22**: 64-QAM 666/1024
** 3GPP TR 38.901 V14.2.0 (2017-09), [1]

5.1 Evaluation metrics

Two metrics are used for performance assessment: the Packet Error Rate (PER) at the satellite receiver and the throughput loss due to guard bands. The PER is defined as the ratio between the number of correctly decoded slots on the total number of transmitted slots. The numbers of slots per frame are recalled in Table 5-1. Due to the long Round Trip Time (RTT) in satellite systems, the retransmission of badly decoded packets using Hybrid Automatic Repeat Request (HARQ) may be not always possible. The PER at the first (and unique) transmission must therefore be very low. In this study we set the target PER to 10^{-3}.

5.2 Results

For performance assessment, the Carrier to Noise Ratio (CNR) required to reach the target PER is first measured, without interference. Then the PER with interference for the same CNR is assessed, for different values of the guard band, and for different interfering received powers. The interference is simulated on both sides of the satellite spectrum, see Figure 5-2.

5.2.1 Highway

The performance in the highway scenario, see Table 5-2, are evaluated in this section. The CNRs required for reaching the target PER without interference are given in Table 5-3.

- Whatever the numerology and the MCS, the required CNR is lower for the 30.72 MHz bandwidth than for the 15.36 MHz bandwidth (between 1.35 and 0.2 dB). This is due to the fact that the code word is twice as long in the former case than in the latter (therefore performance are better).
- Whatever the bandwidth and the MCS, the required CNR for numerology 2 is a bit lower than for numerology 3 (between 0.75 and 0.1 dB): similarly to the previous case, the code word is twice as long for numerology 2 than for numerology 3.

Table 5-3: Required CNR for reaching target PER without interference, highway scenario

MCS	μ	Bandwidth (MHz)	CNR (dB)
15	2	15.36	19
		30.72	18.8
	3	15.36	19.8
		30.72	18.9
10	2	15.36	15.35
		30.72	14
	3	15.36	15.5
		30.72	14.7
5	2	15.36	10.25
		30.72	9.85
	3	15.36	11
		30.72	10.4

Figure 5-3 shows the performance for MCS15, for 15.36 MHz (on the left) and 30.72 MHz (on the right) bandwidths. Even with a huge guard band (980 kHz), if the interferer received power is 10 dB (or more) higher than the satellite received power, the performance is dramatically affected (PER four times higher than target in the best case). Unfortunately, referring to Figure 5-1, this situation happens most of the time. For ΔP=5 dB, the target PER is nearly reached only for numerology 2 and 15.36 MHz band, but with the maximal tested guard band. The only situation where the target PER is reached is when the received powers are equivalent and for numerology 2 / 15.36 MHz band. According to Figure 5-1, ΔP=0 dB only happens in dry weather and when the UE is far away from the interfering gNB.

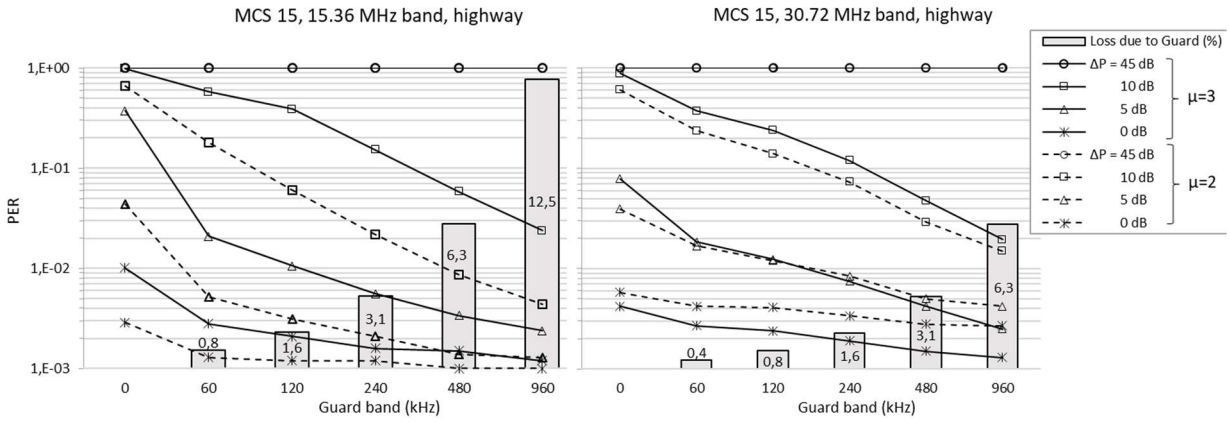

Figure 5-3: MCS 15, highway scenario. Left: 15.36 MHz band; right: 30.72 MHz band

Figure 5-4 shows the performance for MCS10, for 15.36 MHz (on the left) and 30.72 MHz (on the right) bandwidths. For ΔP>10 dB, i.e. most of the time according to Figure 5-1, a very high guard band (960 kHz) is necessary – but not sufficient – to approach the target PER. If the interferer received power is 5 dB higher than the satellite received power, therefore it is possible to use numerology 2, but with a 480 kHz guard band. The only situation where the required guard band is reasonably small is for ΔP=0: 120 kHz are enough to reach PER=10^{-3}, for the 15.36 MHz band.

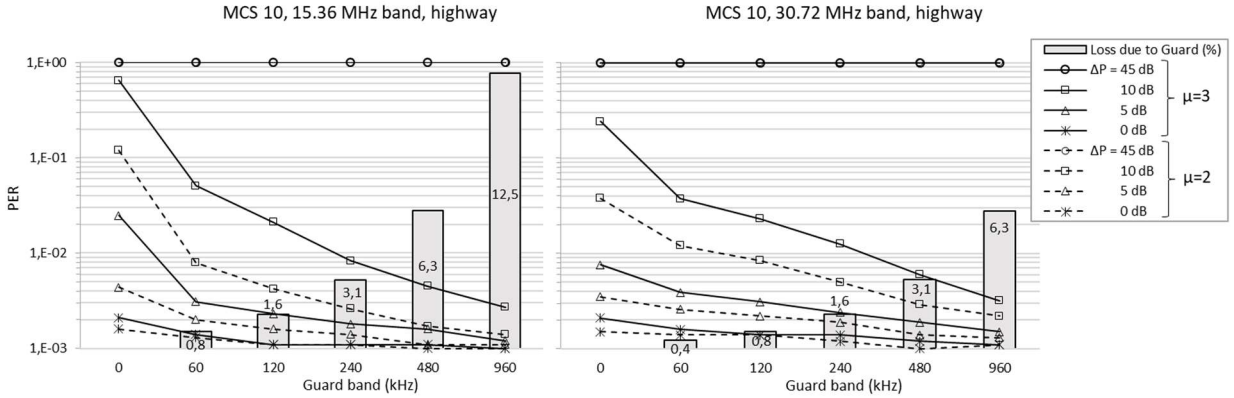

Figure 5-4: MCS 10, highway scenario. Left: 15.36 MHz band; right: 30.72 MHz band

The results for the most robust MCS, #5, are presented in Figure 5-5. The impact of the interference is lower than for higher MCS, even if it is still mandatory that ΔP is lower than 10 dB. If ΔP=5 dB, a 240 kHz may be enough to nearly reach the target PER. The significant result is that for ΔP=0 dB and a 30.72 MHz band, even with no guard band the performance are comparable to that without interference.

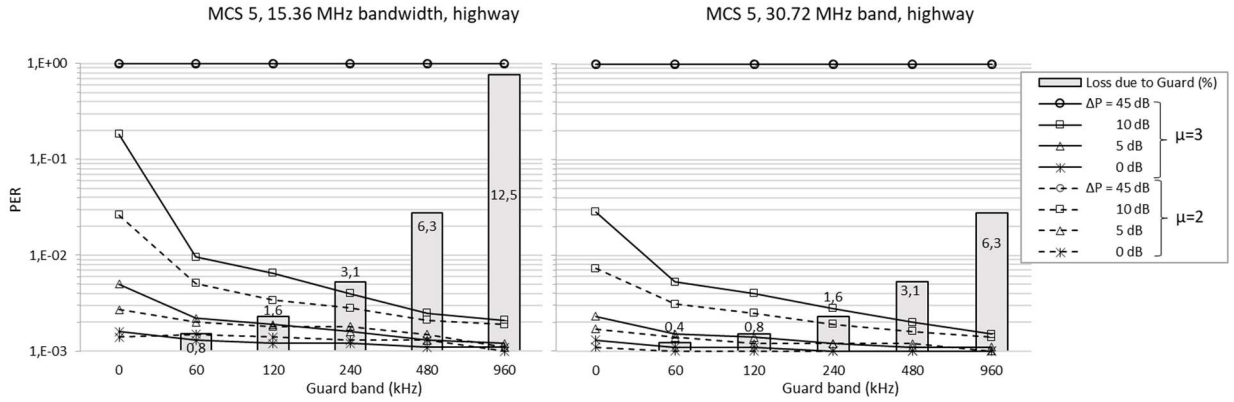

Figure 5-5: MCS 5, highway scenario. Left: 15.36 MHz band; right: 30.72 MHz band

The results for the highway scenario, shown in Figure 5-3 to Figure 5-5, suggest that the received power from the interferer is at least 10 dB higher than the received power from the satellite. Hence, the impact of the interference cannot even be mitigated by the insertion of large guard bands. Unfortunately, this configuration happens most of the time. In presence of adjacent channel interference, a transmission to the satellite user is possible, by carefully choosing the MCS and the guard band, even if ΔP is below 5 dB.

5.2.2 Urban

The performance in the urban scenario, see Table 5-2, are evaluated in this section. The CNRs required for reaching the target PER without interference are given in Table 5-4. Similarly to the highway scenario, the CNR required for numerology 2 is lower than for numerology 3, due to the longer code word for the former.

Table 5-4: Required CNR for reaching target PER without interference, urban scenario

MCS	μ	CNR (dB)
5	2	19.5
	3	21.5
2	2	15.65
	3	18.5

Performance for MCS5 are shown on Figure 5-6. If ΔP≥10 dB the target PER cannot be reached, even it is approached for a 960 kHz guard band and numerology 2. If ΔP≤5 dB, a 240 kHz guard band allows the cancellation of the effect of interference.

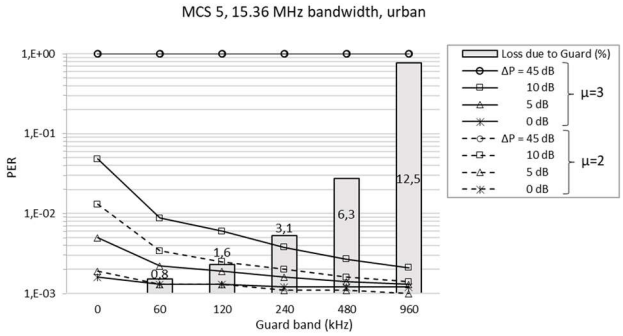

Figure 5-6: MCS 5, urban scenario. 15.36 MHz band

Figure 5-7 presents the results for the most robust of all the assessed MCS. Once again ΔP must be higher than 10 dB. For ΔP=5 dB, 240 kHz guard band is enough. If the powers received from the satellite and from the interfering gNB are equivalent, it is possible to transmit without guard band.

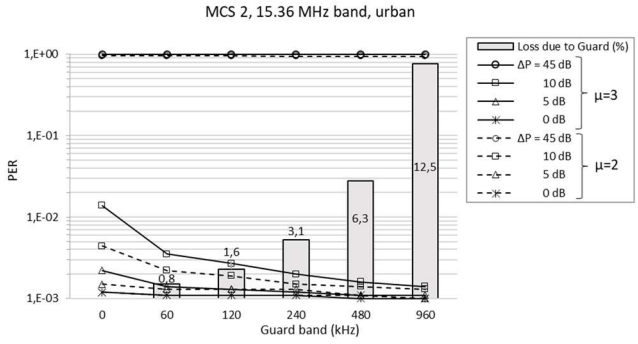

Figure 5-7: MCS 2, urban scenario.15.36 MHz band

The conclusions for the urban scenario are similar to the ones for the highway scenario: in any case, the power received from the interferer must not be more than 10 dB higher than the power of the signal of interest. In view of Figure 5-1, this situation is not very likely.

6 Conclusions

The report discussed the interference situations that are considered in this project. It could be differentiated between the interference that is caused by the non-terrestrial system onto the terrestrial system and the interference that is caused by the terrestrial system onto the non-terrestrial system. Types of interferers and victims were also introduced and the interference could be categorized into co-channel and adjacent channel interference.

The analysis of co-channel interference was based on the channel models that were developed at the beginning of the project. In addition, an outage probability analysis and a stochastic geometry-based analysis was conducted.

The theoretically derived outage probability analysis for the considered scenarios could be verified by simulations. In addition, the results show that the interference leads to higher outage probabilities, especially in the low SNR/SIR threshold region.

The stochastic geometry-based analysis suggests that the elevation angle of the satellite earth station is one of the most important factors that affect the interference at the SES due to the nearby located BSs. It could also be shown that an increasing exclusion zone radius reduces the aggregated interference level, while an increasing BS density leads to an increased interference level. The BS beamwidth also has an effect on the interference at the SES, i.e. the lower the beamwidth the higher the variance of the interference level.

The results of the ray-tracing based analysis show that the C/I at the satellite UE decreases with an increasing attenuation due to rain considering the interference caused by BSs in both considered environments, i.e. urban and highway. This effect is reversed when looking at the cellular UE that is interfered by a satellite. Furthermore, the results indicate that the satellite has almost no impact on the terrestrial system, while the impact from the terrestrial system onto the satellite UEs is significant.

Interference simulations between satellite and terrestrial networks have been done using a geometric-stochastic approach based on QuaDRiGa. UEs could either be assigned to the satellite network or to the cellular network while the other system causes interference. In the S-band, all UEs are hand-held terminals whereas in the Ka-band, VSAT terminals with high-gain antennas are used for satellite access. S-band satellite terminals are severely affected by the interference from the cellular network. Without measures against this interference, coexistence will not be possible. With geometry factors below -25 dB, it might even be difficult to mitigate adjacent channel interference in some cases. On the other side, coexistence at mm-wave frequencies seems feasible due to the narrow beam of the VSAT terminals. However, there is some interference between satellite UEs and cellular gNBs that needs to be taken into account. This is due to the fact that gNBs are at an elevated position and receive more power from (some of) the satellite UEs communicating with their satellite counterpart. This might be more problematic for LEO access at elevation angels below 30° when the UE uses phased array antennas. However, further studies are required to take whole LEO networks with multiple satellites into account.

The study of adjacent channel interference combined with the analysis of received powers from [27] highlights the need for additional signal processing at the waveform level. Considering a satellite UE polluted by a terrestrial gNB, most of the time, even with prohibitive guard bands, the interfering power is too high for a correct transmission. In a future deliverable, we will therefore study filtering techniques at the transmission, in order to mitigate the impact of adjacent channel interference.

The results from this deliverable are expected to contribute to the ongoing and planned works in WP3, WP4, and WP5 of the 5G-ALLSTAR project with the following details:

- WP3: The interference analysis results conducted in D3.2 can provide the design requirement and criteria for formulating and developing specific interference mitigation techniques which will be done in T3.3 and T3.4. The channel model-based simulation

techniques which were further evolved in this deliverable can be reused for the evaluation of the interference mitigation techniques to be developed in T3.3 and T3.4.

- WP4: The implementation of the multi-connectivity algorithms can benefit from the interference analysis results conducted in WP3. The potential severe interference situation between the satellite and terrestrial systems can be considered in the design of the load balancing algorithm.
- WP5: The results provided in this deliverable will be considered for the system setup, frequency usage plan, and deployment of the PoC demonstration in WP5.

7 References

[1] 3GPP TR 38.901, "3rd Generation Partnership Project; Technical Specification Group Radio Access Network; Study on channel model for frequencies from 0.5 to 100 GHz (Release 14)," v14.0.0, Tech. Rep., 2017.

[2] 3GPP TR 38.801, "3rd Generation Partnership Project; Technical Specification Group Radio Access Network; Study on new radio access technology: Radio access architecture and interfaces (Release 14)," v14.0.0, Tech. Rep., 2017.

[3] 3GPP TR 38.811, "3rd Generation Partnership Project; Technical Specification Group Radio Access Network; Study on New Radio (NR) to support non-terrestrial networks (Release 15)," v15.1.0, Tech. Rep., 2019.

[4] 3GPP TR 38.821, "3rd Generation Partnership Project; Technical Specification Group Radio Access Network; Solutions for NR to support non-terrestrial networks (NTN) (Release 16)," v1.0.0, Tech. Rep., 2019.

[5] M. D. Sanctis, E. Cianca, M. Ruggieri, "IP-based routing algorithms for LEO satellite networks in near-polar orbits," IEEE Aerospace Conference Proceedings, Mar. 2003.

[6] A. Ghasemi and E. S. Sousa, "Fundamental limits of spectrum-sharing in fading environments," IEEE Transactions on Wireless Communications, vol. 6, no. 2, pp. 649–658, Feb. 2007.

[7] L. Yang and M.-S. Alouini, "Performance analysis of multiuser selection diversity," IEEE Transactions on Vehicular Technology, vol. 55, no. 6, pp. 1848–1861, Nov. 2006.

[8] P. Viswanath, D. N. C. Tse, and R. Laroia, "Opportunistic beamforming using dumb antennas," IEEE Transactions on Information Theory, vol. 48, no. 6, pp. 1277–1294, Jun. 2002.

[9] D. Tse and P. Viswanath, Fundamentals of Wireless Communication, Cambridge University Press, 2005.

[10] A. Papoulis and S. U. Pillai, Probability, Random Variables and Stochastic Processes, 4th Ed., McGraw-Hill, 2002.

[11] I. S. Gradshteyn and I. M. Ryzhik, Tables of Integrals, Series, and Products, 7th ed. London, UK: Academic Press, 2007.

[12] A. P. Prudnikov, J. A. Bryckov, and O. I. Maricev, Integrals and Series. 3, More Special Functions, Gordon and Breach, 2002.

[13] D. Stoyan, D. Kendall, and J. Mecke, *Stochastic Geometry and Its Applications*. New York: Wiley, 1995.

[14] C. Zhang and W. Zhang, "Spectrum sharing for drone networks," *IEEE J. Sel. Areas Commun.*, vol. 35, no. 1, pp. 136–144, Jan. 2017.

[15] J. G. Andrews, T. Bai, M. N. Kulkarni, A. Alkhateeb, A. K. Gupta, and R. W. Heath, Jr., "Modeling and analyzing millimeter wave cellular systems," *IEEE Trans. Commun.*, vol. 65, no. 1, pp. 403–430, Jan. 2017.

[16] M. Rebato, J. Park, P. Popovski, E. de Carvalho, and M. Zorzi, "Stochastic geometric coverage analysis in mmWave cellular networks with a realistic channel model," in *Proc. IEEE Glob. Commun. Conf. Mobile Wireless Netw. (Globecom MWN)*, Singapore, Dec. 2017.

[17] J. Wildman, P. H. Nardelli, M. Latva-aho, and S. Weber, "On the joint impact of beamwidth and orientation error on throughput in wireless directional Poisson networks," *IEEE Trans. Wireless Commun.*, vol. 13, no. 12, pp. 7072–7085, Dec. 2014.

[18] J. Lyu and R. Zhang, "Network-Connected UAV: 3-D System Modeling and Coverage Performance Analysis," *IEEE Int. Things J.*, vol. 6, no. 4, pp. 7048–7060, Aug. 2019.

[19] V. V. Chetlur and H. S. Dhillon, "Downlink coverage analysis for a finite 3-D wireless network of unmanned aerial vehicles," *IEEE Trans. Commun.*, vol. 65, no. 10, pp. 4543–4558, Jul. 2017.

[20] P. Sharma and D. Kim, "Coverage probability of 3-D mobile UAV networks," *IEEE Wireless Commun. Lett.,* vol. 8, no. 1, pp. 97–100, Feb. 2019.

[21] F. Baccelli and A. Giovanidis, “A stochastic geometry framework for analyzing pairwise-cooperative cellular networks,” *IEEE Trans. Wireless Commun.*, vol. 14, no. 2, pp. 794–808, Feb. 2015.

[22] C. Zhang, C. Jiang, L. Kuang, J. Jin, Y. He, and Z. Han, “Spatial spectrum sharing for satellite and terrestrial communication networks,” *IEEE Trans. Aerosp. Electron. Syst.*, vol. 55, no. 3, pp. 1075–1089, Jun. 2019.

[23] H. Nam, K. S. Ko, I. Bang, and B. C. Jung, “Achievable rate analysis of opportunistic transmission in bursty interference networks,” *IEEE Commun. Lett.*, vol. 22, no. 3, pp. 654–657, Mar. 2018.

[24] C. Balanis, Antenna Theory, Analysis and Design, 3rd ed. Hoboken, NJ, USA: Wiley, 2005.

[25] https://www.ericsson.com/en/blog/2019/1/drones-and-networks-mobility-support

[26] 3GPP S1-193146, “3rd Generation Partnership Project; Performance requirements for satellite access; Change Request (CR) for TS 22.261; (Release 17),” Nov 2019.

[27] 5G-ALLSTAR D3.1, “Spectrum usage analysis and channel model”, June 2019.

[28] https://artes.esa.int/projects/cadsat